4030 *Inorg. Chem.* **1993,** *32,* 4030–4041

Electronic Effects in Transition Metal Porphyrins. 7. Synthesis and Spectroscopic Investigations of a Series of Octasubstituted Porphyrin Isomers and Their Iron(III) Complexes

Meden F. Isaac,[†] Qing Lin,[†] Ursula Simonis,[*,†] Daniel J. Suffian,[†] Debra L. Wilson,[†] and F. Ann Walker[*,‡]

Department of Chemistry and Biochemistry, San Francisco State University,
San Francisco, California 94132, and Department of Chemistry, University of Arizona,
Tucson, Arizona 85721

Received February 26, 1993[⊗]

The synthesis, from a mixture of 3,4-diethylpyrrole, 3,4-bis(*N,N*-diethylcarbamoyl)pyrrole, and formaldehyde, of six pyrrole-substituted porphyrin isomers and their characterization by UV–visible and ^{1}H NMR spectroscopy is reported. Spectral band shifts of the six isomers are irregular, but generally in the order OEPH$_2$ < E$_6$A$_2$PH$_2$ < *t*-E$_4$A$_4$PH$_2$ < *c*-E$_4$A$_4$PH$_2$ > E$_2$A$_6$PH$_2$ > OAPH$_2$ for the four visible bands, while the Soret band shifts to longer wavelengths as diethyl substituents are replaced by carbamoyls. The relative intensities of the visible bands I–IV vary in accord with the predictions of Falk (*Porphyrins and Metalloporphyrins*, Elsevier: New York, 1964), based on the symmetry of the molecules. The ^{1}H NMR spectra of these six free-base porphyrins show the general effects of the ethyl groups in strengthening the ring current relative to the amide groups, but in addition demonstrate the much stronger ring current in the *trans* relative to the *cis* isomer of E$_4$A$_4$PH$_2$. Both the high-spin and low-spin iron(III) complexes of the six pyrrole-substituted porphyrins were also synthesized and characterized by ^{1}H NMR spectroscopy at several temperatures. In all of the low-spin Fe(III) porphyrin isomers, the pattern of spin delocalization within the porphyrin ring is sensitive to both the nature of the substituents and their pattern of substitution. In both high- and low-spin Fe(III) complexes of the mixed substituent porphyrins, the methylene protons of the ethyl substituents exhibit diastereotopism due to the lack of coplanarity of the amide substituents with the porphyrin ring. A combination of COSY and NOESY investigations of [E$_6$A$_2$PFe(*N*-MeIm)$_2$]$^+$ performed at –45 and –60 °C in CD$_2$Cl$_2$ allowed the assignment of all methylene protons of the three unique types of ethyl groups to their respective positions. The EPR spectra of the bis(*N*-methylimidazole) complexes of the same series of compounds show a marked difference between the *cis* and *trans* isomers, with much larger *g* anisotropy for the *trans* isomer than the *cis* ($\Delta g_c = 1.042$; $\Delta g_t = 1.496$, where $\Delta g = g_1 - g_3$). As a consequence of this difference, the calculated rhombicity (V/Δ) of the *cis* isomer is greater than $^2/_3$, if it is assumed that $g_1 = g_{zz}$, $g_2 = g_{yy}$, and $g_3 = g_{xx}$. The EPR parameters of *cis*-[E$_4$A$_4$PFe(*N*-MeIm)$_2$]$^+$ suggest that the principal magnetic axis may be in the plane of the macrocyclic ring, at least at 8 K.

Introduction

Since the pioneering work of Falk in the early 1960s[1] the effects of pyrrole substitution on the electronic properties of porphyrins and metalloporphyrins have been of interest to chemists and biochemists. Extensive studies of the electronic absorption spectra of natural porphyrins and their derivatives by Falk,[1] Caughey and co-workers,[2] Longuet-Higgins,[3] Gouterman,[4–6] and Platt[7] have led to both empirical correlations and theoretical predictions concerning the effect of electron-withdrawing or -donating substituents, and the symmetry of placement of those substituents on the positions and relative intensities of electronic absorption bands. Likewise, ^{1}H NMR investigations by Caughey,[8] Abraham,[9] and others have shown the importance of the nature and pattern of pyrrole substitution on the ring current shifts of free base porphyrins. Investigations by a number of research groups, which have been summarized in two extensive reviews,[10,11] have demonstrated the importance of β-pyrrole and *meso* substituents on the contact shifts of both high- and low-spin iron(III) porphyrins.

Because most of the natural porphyrins investigated to date are unsymmetrically substituted, it is sometimes difficult to relate the changes observed in electronic absorption and ^{1}H NMR spectra to changes in the electronic effects of substituents, as distinguished from changes in symmetry alone. To circumvent this problem, many workers (including the present authors) have turned to symmetrical tetraphenylporphyrins and have investigated in detail the effects of phenyl substituents on the physical and chemical properties of tetraphenylporphyrins and their metal complexes.[10–19] Such studies have been further extended in our laboratories to include detailed investigations of unsymmetrically phenyl-substituted tetraphenylporphyrins and their metal

---

[†] San Francisco State University.
[‡] University of Arizona.
[⊗] Abstract published in *Advance ACS Abstracts,* September 1, 1993.

(1) Falk, J. E. *Porphyrins and Metalloporphyrins*; Elsevier: New York, 1964.
(2) Caughey, W.; Fujimoto, W.; Johnson, B. *Biochemistry* **1966,** *5,* 3830.
(3) Longuet-Higgins, H. C.; Rector, C. W.; Platt, J. R. *J. Chem. Phys.* **1950,** *18,* 1174.
(4) Gouterman, M. *J. Chem. Phys.* **1959,** *30,* 1139.
(5) Gouterman, M. *J. Mol. Spectrosc.* **1961,** *6,* 138.
(6) Gouterman, M. In *The Porphyrins*; Dolphin, D., Ed.; Academic Press: New York, 1978; Vol. III, pp 1–165.
(7) Platt, J. R. In *Radiation Biology*; Hollaender, A., Ed.; McGraw Hill: New York, 1956; Vol. 3, p 96.
(8) Caughey, W.; Koski, W. *Biochemistry* **1952,** *5,* 923.
(9) Abraham, J. R.; Jackman, L. M. *J. Chem. Soc.* **1956,** 1172.
(10) LaMar, G. N.; Walker, F. A. In *The Porphyrins*; Dolphin, D., Ed.; Academic Press: New York, 1979; Vol. IV, pp 61–157.
(11) Walker, F. A.; Simonis, U. Proton NMR Spectroscopy of Model Hemes. In *NMR of Paramagnetic Molecules*; Berliner, L. J., Reuben, J., Eds.; Plenum: New York, 1993; Vol. 12, pp 133–274.
(12) Meot-Ner, M.; Adler, A. D. *J. Am. Chem. Soc.* **1975,** *97,* 5107.
(13) Janson, T. R.; Katz, J. J. In *The Porphyrins*; Dolphin, D., Ed.; Academic Press: New York, 1979; Vol. IV, pp 1–59 and references therein.
(14) Eaton, S. S.; Eaton, G. R. *J. Am. Chem. Soc.* **1977,** *99,* 6594.
(15) Walker, F. A.; Hui, E.; Walker, J. M. *J. Am. Chem. Soc.* **1975,** *97,* 2390.
(16) Walker, F. A.; Beroiz, D.; Kadish, K. M. *J. Am. Chem. Soc.* **1976,** *98,* 3484.
(17) Walker, F. A.; Lo, M.-W.; Ree, M. T. *J. Am. Chem. Soc.* **1976,** *98,* 5552.
(18) Satterlee, J. D.; LaMar, G. N.; Frye, J. S. *J. Am. Chem. Soc.* **1976,** *98,* 7275.

0020-1669/93/1332-4030$04.00/0

complexes.[19–24] While electronic absorption spectral shifts do not appear to follow clear-cut trends for all isomers, the ^{1}H NMR spectra of the series of six isomers of $(p\text{-Cl})_n(p\text{-NEt}_2)_{4-n}\mathrm{TPPH_2}$[20] and their respective Zn(II)[20] and low-spin Fe(III) complexes[24] were rich in information concerning the porphyrin ring current in the free base and zinc complex isomers[20] and the pattern of spin delocalization in the iron complexes.[24] However, several problems have been encountered in our investigations of unsymmetrically substituted *meso*-tetraphenylporphyrins and their metal complexes that have led us back to the investigation of pyrrole-substituted porphyrins. These problems include (1) the question of whether the phenyl substituents interact with the porphyrin ring by means of induction or resonance, or a combination of the two, (2) the fact that *meso* substitution does not provide the optimal symmetry for consideration of the interaction of metal d_π orbitals with the porphyrin nitrogens, and (3) the fact that *meso* substitution does not occur in the natural porphyrins. For these reasons, we have designed a series of high-symmetry β-pyrrole-substituted porphyrins, discussed herein, that have allowed us to probe both electron-donating and -withdrawing effects of β substituents and the effect of the symmetry of placement of these substituents.

With regard to the question of induction or resonance, studies of *meso*-tetraphenylporphyrins and their metal complexes have suggested that for the free bases and divalent metal complexes, the phenyl substituents interact largely by induction.[15,16,21] In contrast, it appears that for trivalent metal complexes, particularly those in which the metal carries a formal positive charge (thus leading to large electron demand at the metal center), interaction of the phenyl substituents through resonance is very important.[22]

With regard to the question of symmetry, it should be recalled that in the case of paramagnetic metalloporphyrins, it is either the $3e(\pi)$ porphyrin filled molecular orbitals[3] or the $4e(\pi^*)$ empty molecular orbitals[3] that have the proper symmetry to overlap with the metal d_π orbitals, d_{xz} and d_{yz}, which are also of e_g symmetry.[10,11] In the case of low-spin Fe(III), the $3e(\pi)$ orbitals, as drawn originally by Longuet-Higgins *et al.*[3] and by Gouterman,[4–6] have a node passing through opposite pyrrole nitrogens, giving rise to $e(\pi_x)$ and $e(\pi_y)$ degenerate orbitals. For these orbitals to be relevant to *meso*-substituted porphyrin isomers, we found it necessary to construct linear combinations of these orbitals,[11,25–27] having nodes passing through opposite *meso* positions, and corresponding linear combinations of d_{xz} and d_{yz}. While this approach is useful in some cases, including several upon which we have recently reported,[27–30] it is not always the most useful, since one would usually like to think of metal d orbitals in relation to Cartesian axes and the porphyrin nitrogen ligand atoms lying on those axes.

In order to demonstrate the effects of electron-donating and -withdrawing substituents on the electronic properties of pyrrole-substituted porphyrins, we have prepared a series of pyrrole-substituted porphyrin isomers, **8a–f**, shown in Figure 1,[31] in which each individual pyrrole ring carried two identical substituents. These isomers are of higher symmetry than any of the naturally-occurring porphyrins. Two recent developments in porphyrin synthetic methods made possible this proposed project: (1) the use of tosylmethyl isocyanide to prepare 3,4-disubstituted pyrroles in good yield[32,33] and (2) the demonstrated synthesis of octakis(*N*,*N*-diethylcarbamoyl)porphyrin,[34] herein called $\mathrm{OAPH_2}$.[31] The free base porphyrins, as well as their corresponding iron(III) porphyrin complexes, have been characterized by UV–visible and ^{1}H NMR spectroscopy, which will be discussed in detail below. We will further demonstrate that the assignment of the NMR resonances of the low-spin Fe(III) complex of the 1,2-bis(*N*,*N*-diethylcarbamoyl)-3,4,5,6,7,8-hexaethylporphyrin isomer, herein called $\mathrm{E_6A_2P}$,[31] by COSY and NOESY techniques, provides valuable information concerning the spin density distribution in this complex. The results are in agreement with our expectations, based upon *meso*-substituted model hemes, and can hence provide a basis for comparison to the naturally-occurring hemes.

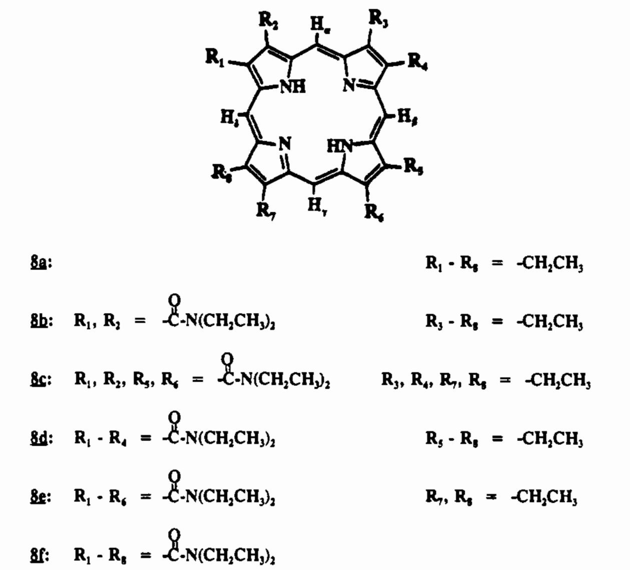

8a: $R_1 - R_8 = -CH_2CH_3$

8b: $R_1, R_2 = -\overset{O}{\overset{\|}{C}}-N(CH_2CH_3)_2$ $R_3 - R_8 = -CH_2CH_3$

8c: $R_1, R_2, R_5, R_6 = -\overset{O}{\overset{\|}{C}}-N(CH_2CH_3)_2$ $R_3, R_4, R_7, R_8 = -CH_2CH_3$

8d: $R_1 - R_4 = -\overset{O}{\overset{\|}{C}}-N(CH_2CH_3)_2$ $R_5 - R_8 = -CH_2CH_3$

8e: $R_1 - R_6 = -\overset{O}{\overset{\|}{C}}-N(CH_2CH_3)_2$ $R_7, R_8 = -CH_2CH_3$

8f: $R_1 - R_8 = -\overset{O}{\overset{\|}{C}}-N(CH_2CH_3)_2$

Figure 1. Structures of the six isomers of this study. In the simplified names, E represents ethyl and A represents *N*,*N*-diethylcarbamoyl.

Experimental Section

Materials and Methods. Reagents for the synthesis of the pyrroles **1**, **4**, and **7** were purchased from Aldrich and used as received. All solvents (HPLC or Optima grade, Fisher Scientific) were used without purification except as follows: Diethyl ether was distilled over sodium using benzophenone as indicator. Benzene, methylene chloride, and tetrahydrofuran were distilled over $\mathrm{CaH_2}$ immediately before use. Dimethyl sulfoxide was distilled over $\mathrm{CaH_2}$ under reduced pressure and stored over molecular sieves (Linde 4 Å). Diethylamine was distilled before use. Silica gel (60–200 mesh) from J. T. Baker and basic alumina from Fischer were used for column chromatography. HPLC separation of the *cis* and *trans* isomers was achieved utilizing an Altex-Beckman Model 110B

---

(19) Walker, F. A.; Reis, D.; Balke, V. L. *J. Am. Chem. Soc.* **1984**, *106*, 6888.

(20) Walker, F. A.; Balke, V. L.; McDermott, G. A. *Inorg. Chem.* **1982**, *21*, 3342.

(21) McDermott, G. A.; Walker, F. A. *Inorg. Chim. Acta* **1984**, *91*, 95.

(22) Balke, V. L.; Walker, F. A.; West, J. T. *J. Am. Chem. Soc.* **1985**, *107*, 1226.

(23) Walker, F. A.; Barry, J. A.; Balke, V. L.; McDermott, G. A.; Wu, M. Z.; Linde, P. F. *Adv. Chem. Ser.* **1982**, *201*, 377.

(24) Walker, F. A.; Balke, V. L.; McDermott, G. A. *J. Am. Chem. Soc.* **1982**, *104*, 1569.

(25) Walker, F. A. *J. Am. Chem. Soc.* **1980**, *102*, 3254.

(26) Walker, F. A.; Benson, M. *J. Phys. Chem.* **1982**, *86*, 3495.

(27) Lin, Q.; Simonis, U.; Tipton, A. R.; Norvell, C. J.; Walker, F. A. *Inorg. Chem.* **1992**, *31*, 4216.

(28) Zhang, H.; Simonis, U.; Walker, F. A. *J. Am. Chem. Soc.* **1990**, *112*, 6124.

(29) Walker, F. A.; Simonis, U.; Zhang, H.; Walker, J. M.; Ruscitti, T. M.; Kipp, C.; Amputch, M. A.; Castillo, B. V., III; Cody, S. H.; Wilson, D. L.; Graul, R. E.; Yong, G. J.; Tobin, K.; West, J. T.; Baricheivich, B. A. *New J. Chem.* **1992**, *16*, 609.

(30) Simonis, U.; Dallas, J. L.; Walker, F. A. *Inorg. Chem.* **1992**, *31*, 5349.

(31) Abbreviations used: **8a**, 1,2,3,4,5,6,7,8-octaethylporphyrin, $\mathrm{OEPH_2}$ and its iron(III) complex $\mathrm{(OEP)Fe^{III}}^{+}$; **8b**, 1,2-bis(*N*,*N*-diethylcarbamoyl)-3,4,5,6,7,8-hexaethylporphyrin, $\mathrm{E_6A_2PH_2}$, and its iron(III) complex $\mathrm{E_6A_2PFe^{III}}^{+}$; **8c**, *trans*-1,2,5,6-tetrakis(*N*,*N*-diethylcarbamoyl)-3,4,7,8-tetraethylporphyrin, $t\text{-}\mathrm{E_4A_4Ph_2}$, and its iron(III) complex $t\text{-}\mathrm{E_4A_4PFe^{III}}^{+}$; **8d**, *cis*-1,2,3,4-tetrakis(*N*,*N*-diethylcarbamoyl)-5,6,7,8-tetraethylporphyrin, $c\text{-}\mathrm{E_4A_4PH_2}$, and its iron(III) complex $c\text{-}\mathrm{E_4A_4PFe(III)}^{+}$; **8e**, 1,2,3,4,5,6-hexakis(*N*,*N*-diethylcarbamoyl)-7,8-diethylporphyrin, $\mathrm{E_2A_6PH_2}$, and its iron(III) complex $\mathrm{E_2A_6PFe^{III}}^{+}$; **8f**, 1,2,3,4,5,6,7,8-octakis(*N*,*N*-diethylcarbamoyl)porphyrin, $\mathrm{OAPH_2}$, and its iron(III) complex $\mathrm{(OAP)Fe^{III}}^{+}$; *N*-methylimidazole, *N*-MeIm; imidazole, ImH.

(32) Van Leusen, A. M.; Siderius, H.; Hoogenboom, B. E.; Van Leusen, D. *Tetrahedron Lett.* **1972**, *52*, 5337.

(33) (a) Chamberlin, K. S.; LeGoff, E. *Synth. Commun.* **1978**, *8*, 579. (b) Chamberlin, K. S.; LeGoff, E. *Heterocycles* **1979**, *12*, 1567.

(34) Shirazi, A.; Marianelli, R.; Sturgeon, G. *Inorg. Chim. Acta* **1983**, *72*, 5.

Table I. UV–Visible Spectral Data for the Six Octasubstituted Porphyrins in Methylene Chloride Solution

	λ, nm (ϵ, M^{-1} cm^{-1})				
compound	Soret	IV	III	II	I
$OEPH_3$	398 (1.61×10^5)	498 (1.32×10^4)	532 (1.04×10^4)	566 (6.91×10^3)	620 (4.9×10^3)
$E_6A_2PH_2$	404 (2.92×10^4)	506 (1.54×10^3)	542 (2.24×10^3)	566 (1.32×10^3)	618 (1.40×10^2)
t-$E_4A_4PH_2$	404 (1.71×10^5)	512 (5.24×10^3)	550 (1.41×10^4)	568 (9.4×10^3)	620 (6.6×10^2)
c-$E_4A_4PH_2$	410 (1.68×10^5)	516 (6.63×10^3)	556 (1.02×10^4)	578 (6.9×10^3)	630 (2.01×10^3)
$E_2A_6PH_2$	412 (9.5×10^4)	510 (5.53×10^3)	549 (4.97×10^3)	574 (3.24×10^3)	629 (4.5×10^2)
$OAPH_2$	414 (1.00×10^5)	508 (6.5×10^3)	540 (2.79×10^3)	580 (2.41×10^3)	632 (9.9×10^2)

medium-pressure liquid chromatograph and a reverse phase C_{18} column (Beckman). The sample of mixed isomers was dissolved in methanol, and 100-μL portions were injected for each separation. Each sample was run for 1 h with $MeOH:H_2O$ = 80:20 and then eluted with $MeOH:H_2O$ = 90:10. Fractions (2 mL) were collected. The *trans* isomer eluted first.

UV–visible absorption spectra for the porphyrins **8a–f** dissolved in HPLC grade methylene chloride (Fischer) were recorded on a Hewlett-Packard 8451A spectrophotometer at room temperature. Both 1-D and COSY proton NMR spectra were recorded on a General Electric QE-300 NMR spectrometer operating at 300.15 MHz. Samples were locked on solvent deuterium and referenced to residual solvent protons. Both 1- and 2-D (COSY and NOESY) spectra at various temperatures were recorded on a General Electric GN-300 WB NMR spectrometer operating at 300.10 MHz. NMR solvents most frequently used, deuteriochloroform, deuteriomethylene chloride, deuteriobenzene, and deuteriopyridine, and carbon disulfide, were purchased from Aldrich or Cambridge Isotopes. EPR spectra were recorded on a Varian E-12 EPR spectrometer operating at X-band and equipped with an Air Products liquid helium temperature controller. The frequency was calibrated for each run with the Varian weak pitch sample ($g = 2.0027$), and the field sweep was calibrated by use of an NMR gaussmeter.

COSY spectra of the low-spin iron(III) bis(*N*-methylimidazole) complex of **8b** were recorded in CD_2Cl_2 at –45 °C on the General Electric GH-300 WB spectrometer using 128 t_1 blocks of 128 scans each over a spectral bandwidth of 12.99 kHz (12 987 Hz) and 1024 t_2 data points. Data were processed with an unshifted sine–bell–squared window function in both dimensions, zero-filled once in t_1 to yield a final matrix of 512 $t_1 \times 512$ t_2 data points prior to Fourier transformation, magnitude calculation, and symmetrization. NOESY spectra of the same complex were recorded in CD_2Cl_2 at temperatures low enough to suppress axial ligand exchange, namely at –45 and –60 °C, on the same spectrometer using 128 t_1 blocks of 256 scans each over a bandwidth of 8.8 kHz and 512 t_2 data points. The data sets were obtained using the typical 90–t_1–90–τ_m–90–t_2 pulse sequence with a composite 180° pulse applied during the mixing period to suppress unwanted cross peaks arising from scalar couplings. The mixing times at each temperature were varied from 21 to 100 ms and optimized by trial and error to give maximum cross peak intensity. Data were processed with an unshifted sine–bell window function in both dimensions, zero-filled once to 256 $t_1 \times 256$ t_2 data points prior to Fourier transformation, magnitude calculation, and symmetrization.

Synthetic Procedures. Dimethyl-3,4-pyrroledicarboxylate **1** was synthesized from dimethyl maleate and (*p*-tolylsulfonyl)methyl isocyanide (TosMIC),[30] hydrolyzed to the free diacid **2**,[31] converted to the corresponding diacid chloride **3**,[31] and reacted with diethylamine[32] according to literature procedures, with some modifications. Complete procedures are given in the supplementary material and in the M.S. Thesis of Isaac.[35] The crude product was recrystallized from benzene to yield 3,4-bis(*N,N*-diethylcarbamoyl)pyrrole, **4**, in overall yield of 32%. ^1H NMR ($CDCl_3$), δ (ppm): 1.08 (12H, t, amide CH_3), 3.43 (8H, q, amide CH_2–), 6.74 (2H, s, α-Pyr–H), 10.30 (1H, s(br), N–H). The 3,4-diethylpyrrole, **7**, was prepared as described previously,[33] with some modifications, and used immediately. Complete procedures are given in the supplementary material and in the M.S. Thesis of Isaac.[35] ^1H NMR ($CDCl_3$), δ (ppm): 1.20 (6H, t, CH_3), 2.46 (4H, q, CH_2–), 6.52 (2H, d, α-Pyr–H), 8.0 (1H, s(br), N–H). NMR spectra showed traces of THF solvent at 1.85 (2H) and 3.75 ppm (2H) and no observable (≪1%) starting material.

Octasubstituted Porphyrins 8a–f.[34] A solution of 3,4-bis(*N,N*-diethylcarbamoyl)pyrrole **4** (4.4 g, 17.2 mmol), crude 3,4-diethylpyrrole **7** (2.1 g, 17.2 mmol), 128 mL of 37% formaldehyde, 32 mL of 48% HBr, and 1.28 L of absolute ethanol was heated under gentle reflux while stirring for 24 h in an inert N_2 atmosphere. The solution was then refluxed for another 24 h while exposed to air. The resulting black solution was cooled to room temperature and transferred to a beaker which was exposed to air for 15 days. The thick black mixture was dissolved in a small amount of ethanol and then neutralized with 1 M KOH, 400 mL of H_2O was added, and the solution was extracted with CH_2Cl_2 (3 × 75-mL aliquots). The methylene chloride extract was filtered and reduced in volume. The residue was chromatographed on a silica gel gravity flow column (3 × 125 cm) and eluted with toluene, toluene–methylene chloride, methylene chloride, methylene chloride–ethyl acetate, ethyl acetate, and ethyl acetate–methanol (3%). Fractions were collected and checked by TLC and UV–visible spectrophotometry. Pure fractions were dried under vacuum and ^1H NMR spectra were recorded. Yields and optimum elution solvents (in parentheses): $OEPH_2$ (**8a**), 11.0% (40% CH_2Cl_2, 60% toluene); $E_6A_2PH_2$ (**8b**), 0.24% (5% EtOAc, 95% CH_2Cl_2); *t*-, *c*-$E_4A_4PH_2$ (**8c**, **8d**), 1.0% combined, 0.7%, 0.3% by NMR (25% EtOAc, 75% CH_2Cl_2 as combined bands on silica gel); $E_2A_6PH_2$ (**8e**), 0.08% (EtOAc); $OAPH_2$ (**8f**), trace (3% MeOH, 97% EtOAc).

The *cis* and *trans* isomers of $Et_4A_4PH_2$ could not be separated by gravity flow chromatography using silica gel or alumina as the solid support. They were therefore separated in small quantities by HPLC utilizing a Beckman reverse phase C_{18} column, and $MeOH/H_2O$ solvent mixtures (80:20 followed by 90:10). The *cis* isomer, *c*-$E_4A_4PH_2$ appeared to be relatively unstable, with greenish, unidentified products being isolated by HPLC after every run; hence, the yield of *cis* isomer decreased upon passage through the HPLC column, and pure *cis* isomer could not be obtained. Optical and ^1H NMR studies were thus conducted on either the original mixture of the two isomers or a small sample of a 16:1 ratio of *cis*:*trans*-$E_4A_4PH_2$. UV–visible spectral data of the six porphyrin isomers are summarized in Table I, and ^1H NMR data, in Table II. Octaethylporphyrin, $OEPH_2$ (**8a**),[33] and octakis(*N,N*-diethylcarbamoyl)-porphyrin, $OAPH_2$ (**8f**),[34] were separately synthesized and obtained as pure isomers as previously reported, with some modifications. Complete procedures are provided in the supplementary material and in the M.S. Thesis of Isaac.[35]

Iron(III) Porphyrins.[36] Each pure porphyrin product (0.02 mmol) was dissolved in hot DMF (10 mL). The solution was allowed to reflux while stirring. After a few minutes a stoichiometric amount of $FeBr_2$ was added. The reaction was allowed to reflux and the extent of metalation was monitored by the change in the four visible bands of the porphyrin (I–IV) into two bands. If necessary, after about 10 min, an additional half of the stoichiometric amount of $FeBr_2$ was added. The reaction mixture was allowed to cool and an equal volume of CH_2Cl_2 was added. It was then transferred to a separatory funnel containing 200 mL of water. The organic layer was separated without shaking to avoid the formation of an emulsion. The organic layer was washed several times with 200 mL of water to remove traces of DMF. The CH_2Cl_2 extracts were reduced in volume and put onto a silica gel column (2 × 25 cm). Traces of unmetalated porphyrin eluted first, and the greenish-brown nonfluorescent band of the metallated porphyrin was eluted with 5% methanol in CH_2Cl_2 and collected. The solution was evaporated to dryness and redissolved in benzene, and HCl gas was bubbled through the solution to reverse μ-oxo dimer formation. The solvent was then evaporated. ^1H NMR spectra of the high-spin iron porphyrins were recorded in $CDCl_3$ at 25 °C.

Iron(III) Porphyrin Bis(*N*-methylimidazole) Complexes. To an NMR tube containing each (porphyrin)FeCl isomer, aliquots of *N*-methylimidazole (*N*-MeIm) (Aldrich) were added until the resonances corresponding to the high-spin complex diasppeared to leave only the peaks corresponding to the low-spin iron(III) porphyrin complex. The ^1H NMR spectra were recorded in $CDCl_3$ at temperature intervals of 10 °C and in one case in CD_2Cl_2. EPR spectra were obtained at 8 K after transfer of the $CDCl_3$ NMR samples to 4-mm quartz EPR tubes.

---

(35) Isaac, M. F. M.S. Thesis, San Francisco State University, 1988.

(36) Adler, A. D.; Longo, F. R.; Kampas, F.; Kim, J. *J. Inorg. Nucl. Chem.* **1970**, *32*, 2443.

Table II. Proton NMR Chemical Shifts, δ, in ppm, of the Six Octasubstituted Porphyrins[a]

porphyrin	*meso*-H	N–H	–*CH*$_2$CH$_3$	–CH$_2$*CH*$_3$	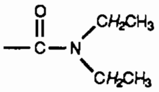	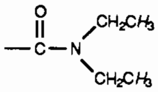
OEPH$_2$	10.15 (4H, s)	–3.73 (2H, s)	4.10 (16H, q)	1.90 (24H, t)		
E$_6$A$_2$PH$_2$	10.11 (2H, s) 10.07 (2H, s)	–3.73 (2H, s)	4.18 (4H, m) 4.03 (8H, m)	1.94 (18H, m)	4.18 (4H, m) 3.72 (2H, m) 3.61 (2H, m)	1.72 (6H, t) 1.06 (6H, t)
t-E$_4$A$_4$PH$_2$	10.12 (4H, s)	–3.82 (2H, s)	3.97 (8H, m)	1.92 (12H, t)	4.13 (8H, m) 3.73 (4H, bm) 3.60 (4H, m)	1.72 (12H, t) 1.07 (12H, t)
c-E$_4$A$_4$PH$_2$	10.07 (10.04[b]) (1H, s) 9.97 (9.94[b]) (1H, s) 9.87 (9.84[b]) (1H, s) ... (9.25[b]) (0.8H, s)	–2.99 (–3.02[b]) (1H, s) –3.12 (–3.20[b]) (1H, s)	3.97 (8H, m)	1.92 (12H, t)	4.13 (8H, m) 3.70 (8H, bm)	1.72 (12H, t) 1.07 (12H, t)
E$_2$A$_6$PH$_2$	10.07 (4H, bs)	–3.53 (2H, s)	4.06 (4H, m)	1.93 (6H, t)	4.06 (12H, bm) 3.62 (12H, bm)	1.70 (18H, m) 1.06 (18H, m)
OAPH$_2$	10.08 (4H, s)	–3.37 (2H, s)			3.90 (16H, bq) 3.60 (16H, bq)	1.60 (24H, bm) 1.14 (24H, bm)

[a] Recorded in CDCl$_3$ at room temperature. [b] Chemical shifts of a ~0.05 mM solution in CDCl$_3$.

Results and Discussion

Synthesis of Octasubstituted Porphyrins. Tosylmethyl isocyanide (TosMIC) is a convenient starting material for the synthesis of symmetrical and unsymmetrical 3,4-disubstituted pyrroles, as reported previously.[32,33] A Michael-type addition of tosylmethyl isocyanide with the corresponding α,β-unsaturated ketone or ester yields 3-acetyl-4-ethylpyrrole and dimethyl-3,4-pyrroledicarboxylate, which led to 3,4-diethylpyrrole (**7**) and 3,4-bis(*N*,*N*-diethylcarbamoyl)pyrrole (**4**), respectively. The 3,4-diethylpyrrole was found to decompose much more rapidly than the 3,4-bis(*N*,*N*-diethylcarbamoyl)pyrrole and hence was prepared immediately before its use in the synthesis of the mixed porphyrin isomers.

Condensation of an equimolar mixture of 3,4-diethylpyrrole (**7**) and 3,4-bis(*N*,*N*-diethylcarboxamoyl)pyrrole (**4**) with 2 equiv of aqueous formaldehyde in the presence of an acid gave six β-octa-substituted porphyrins **8a–f**, whose structures are shown in Figure 1.[31] The two pyrrole precursors differ markedly in reactivity. Althoug the statistically-expected ratio of isomers is 1:4:2:4:4:1, OEPH$_2$ was formed readily in highest yield of any of the isomers. The E$_2$A$_6$PH$_2$ isomer was formed in very small yield, and it was necessary to synthesize OAPH$_2$ spearately[34] since only a trace amount of it was observed in the crude mixture. Although the porphyrin isomers were obtained in very low yields, the quantities were sufficient for all spectroscopic chacterizations except those involving the iron complex of the E$_2$A$_6$P isomer.

Two additional porphyrin isomers, termed "P$_2$" and "P$_3$", which eluted just after OEPH$_2$ and well before E$_6$A$_2$PH$_2$, were found to be present in small amounts in some preparations. Since they were isolated only in small quantities, no attempt to structurally characterize them was undertaken. However, it can be assumed that based upon their elution properties, they contained groups less polar than diethylcarbamoyl but more polar than ethyl. From consideration of the synthetic route used for obtaining the 3,4-diethylpyrrole, it is possible that small amounts of the reduced 3-acetyl-4-ethylpyrrole, not detected by ^{1}H NMR spectroscopy, could have reacted to produce porphyrins with one or two acetyl groups instead of ethyls. Indeed, these same porphyrin products were also produced upon synthesis of OEPH$_2$ from the crude 3,4-diethylpyrrole (**7**).

UV–Visible Spectra. The electronic spectral data for the isolated porphyrin free bases are summarized in Table I. The Soret and satellite bands I–IV in the visible region generally shift to longer wavelength as ethyl groups are replaced by electron-withdrawing carbamoyl groups. Spectral band shifts of the six isomers are irregular, but generally in the order OEPH$_3$ < E$_6$A$_2$PH$_2$ < *t*-E$_4$A$_4$PH$_2$ < *c*-E$_4$A$_4$PH$_2$ > E$_2$A$_6$PH$_2$ > OAPH$_2$ for the four visible bands, while the Soret band shifts to longer wavelength as diethyl substituents are replaced by carboxamides. Both OEPH$_2$ (**8a**) and OAPH$_2$ (**8f**) have D_{4h} symmetry if the N–H protons and nonplanar conformations of the β-substituents are ignored, and they exhibit the typical etio-type spectra (IV > III > II > I)[1] observed for all naturally-occurring porphyrins. (In the notation of Falk,[1] the visible bands are numbered I, II, III, and IV in order of increasing energy; in Gouterman's notation the same bands are named $Q_x(0,0)$, $Q_x(1,0)$, $Q_y(0,0)$, and $Q_y(1,0)$.[4–6]) For E$_6$A$_2$PH$_2$ (**8b**) the symmetry is lowered to C_{2v} and the molecule has a rhodo-type spectrum (III > IV > II > I),[1] with band III significantly enhanced and band I reduced in intensity. The two β,β′-diethylcarbamoyls on opposite pyrroles in the *trans*-E$_4$A$_4$PH$_2$ isomer **8c** reinforce the electron-withdrawing effect of each other and an oxorhodo-type spectrum is observed (III > II > IV > I).[1] The *cis*-E$_4$A$_4$PH$_2$ isomer **8d** has a rhodo-type spectrum (III > IV > II > I), although bands II and IV are very similar in intensity. E$_2$A$_6$PH$_2$ (**8e**), which should have a rhodo-type spectrum,[1] as does its reciprocal isomer, actually has an etio-type spectrum (IV > III > II > I), but the intensities of bands IV and III are very similar to each other and intensity of band I is very much reduced relative to those of OEPH$_2$ and OAPH$_2$. Thus E$_2$A$_6$PH$_2$ could be said at least to have a "rhodofied"[1] etio-type spectrum, and it appears that if the symmetry-breaking group is electron-donating, greater effect is observed on the $Q_x(0,0)$ band, I, than on the $Q_y(0,0)$ band, III.

From the extinction coefficients for each of the unsymmetrical porphyrins (Table I), it is evident that bands I and III are the ones most affected by the pattern and degree of substitution. This is consistent with the fact that since bands I and III are classified as the 0–0 forbidden vibronic transitions along the *x* and *y* axes,[6] any loss of symmetry in the molecule has a greater effect on these bands than on bands II and IV, which are due to the allowed 0–1 vibronic excitations. It is furthermore observed that as the symmetry is lowered, the intensity of band III is increased while that of band I is reduced, as compared to the highly-symmetrical porphyrins (OEPH$_2$ and OAPH$_2$) studied. Greater distortion is observed if the symmetry-breaking effect is caused by the introduction of electron-withdrawing groups into a predominantly electron-donating periphery, as in E$_6$A$_2$PH$_2$ (**8b**), or by *trans* location of electron-withdrawing groups. In the four-orbital model of Gouterman,[6] the degenerate e_g levels are transformed into two states called c_1 and c_2 as the symmetry of the porphyrin is lowered by substitution at the porphyrin periphery. As the energy of the two transitions $b_1 \rightarrow c_1$ and $b_2 \rightarrow c_2$ becomes increasingly unequal, the Q_y band gains intensity,[6] which is observed for the octasubstituted porphyrin isomers of the present study.

Proton NMR Spectra of the Free Base Porphyrin Isomers. The ^{1}H NMR chemical shifts of *meso*-H, N–H, and E (pyrrole–

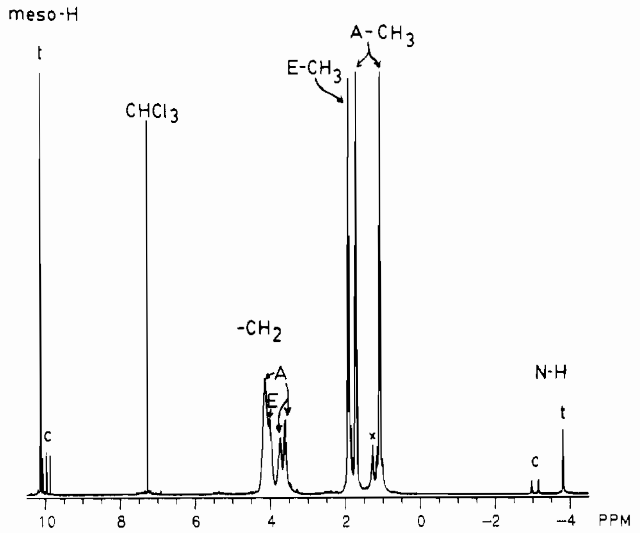

Figure 2. 300-MHz proton NMR spectrum of a 30:70 mixture of the *cis* and *trans* isomers of $E_4A_4PH_2$ in $CDCl_3$ at room temperature.

ethyl) and A (carbamoyl–ethyl) protons are listed in Table II. The mixed pyrrole-substituted isomers reveal resonances whose shifts depend on the number of diethylpyrrole and bis(*N*,*N*-diethylcarbamoyl)pyrrole groups present. The chemical shifts of the *meso* protons are found to be affected by their nearest neighbor pyrrole substituents, as shown in Table II. Methylene and methyl signals from the various ethyl groups present was assigned by homonuclear decoupling and COSY experiments, and those that are coupled are listed on the same line in Table II. The ethyl groups of the carbamoyl substituents (hereafter referred to as A) are nonequivalent, due to restricted rotation about the carbonyl–nitrogen bond. The A–CH_3 groups occur at a lower chemical shift than those of the E–CH_3 substituents, which is seen clearly in $OAPH_2$, $E_2A_6PH_2$, $E_6A_2PH_2$, and *cis*- and *trans*-$E_4A_4PH_2$ (Table II). Thus three methyl signals are observed: two from the amide A– (*syn* and *anti*) and one from the E–ethyl groups. Peaks that correspond to the E–CH_2 overlap with some of the A–CH_2 resonances.

In the case of the mixed *cis*- and *trans*-$E_4A_4PH_2$ isomers, only three *meso*-H peaks were initially observed for the *cis* isomer **8d** at room temperature, of relative intensity 1:1:1 (Figure 2). However, the symmetry of the molecule indicates that there should be four unique *meso*-H signals. To determine whether the fourth *meso*-H resonance of *cis*-$E_4A_4PH_2$ was located under the single *meso*-H resonance of the *trans* isomer, attempts were undertaken to separate the isomers by reverse phase HPLC. Repeated attempts to concentrate the small amounts of the *cis* isomer separated were frustrated by its apparent decomposition upon handling. Green byproducts, which were not characterized, were obtained after every run. Sufficient amounts of 16:1 *cis*:*trans*-$E_4A_4PH_2$ were obtained to allow the UV–visible spectrum to be recorded and a dilute 50-μL sample to be prepared for ^{1}H NMR spectroscopy. As the NMR data were being acquired, it became apparent that there were four *meso*-H peaks from the *cis* isomer at 10.04, 9.94, 9.84, and 9.25 ppm, in addition to the small *meso*-H peak from the *trans* isomer at 10.12 ppm. After 10 min of acquisition, the intensity of the peak at 9.25 ppm was only ~80% of that of each of the other three; after 30 min of acquisition, its intensity had diminished to ~20%. Upon rerecording of the spectrum the next day, the peak at 9.25 ppm could no longer be detected, and the intensities of the remaining three resonances decreased in the order 9.85 > 9.95 > 10.05 ppm. (Initial and final spectra are shown in Figure S-1a,b, supplementary material.) The disappearance of the *meso*-H signal at 9.25 ppm can be easily explained by the commonly observed phenomenom of dueterium substitution in OEP-type model hemes.[37] Due to small amounts of DCl present in $CDCl_3$ the *meso* proton resonating at 9.25 ppm is readily exchanged with deuterium. This exchange seems to be much faster and more favorable than that of the N–H protons, since the intensity of the two N–H resonances decreased to only 34–37% of the expected value (Figure S-1b,c). No attempts were undetaken to back-exchange the deuterium with HCl due to the small amount of material.

H–D exchange has been observed previously by Smith and co-workers for a series of β-substituted porphyrins.[38] It was found that natural porphyrins are differentially deuterated at the *meso* positions by *p*-toluenesulfonic acid-d_1 under seemingly more extreme conditions of higher temperature and higher acid concentration;[38] for zinc(II) protoporphyrin IX dimethyl ester, the rate of deuteration is in the order $\gamma > \delta > \beta > \alpha$, with the reaction requiring 4 days at 80 °C. The extreme ease of substitution of the *meso*-H proton of *cis*-$E_4A_4PH_2$ that resonates at 9.25 ppm, as well as its smaller chemical shift, may be consistent with the fact that the purified *cis* isomer appeared to be somewhat unstable, as evidenced by the green byproducts formed upon purification. It may have undergone degradation to form the oxophlorin, under the influence of oxygen and light, as is known to occur for other non-*meso*-substituted porphyrins.[39]

The order of ease of substitution of the *meso*-H of zinc(II) protoporphyrin IX dimethyl ester[38] has suggested that *meso*-H atoms near electron-donating substituents are more readily exchanged than those near electron-withdrawing groups, presumably because the increased electron density makes the *meso* carbon more basic. By this reasoning, for *cis*-$E_4A_4PH_2$, the peak at 9.25 ppm must be due to H_γ, the *meso*-H between the two pyrrole rings bearing diethyl groups, while the peak at 9.85 ppm is likely H_α, the *meso*-H between the two pyrrole rings bearing *N*,*N*-diethylcarbamoyl groups. It should also be noted that the average *meso*-H shift of *cis*-$E_4A_4PH_2$ (9.77 ppm) (or indeed, even the average of the three closely-spaced *meso*-H peaks) is much less than that of any of the other mixed- or pure-substituent octasubstituted porphyrin isomers (10.07–10.15 ppm), suggesting that the porphyrin ring current is less strong in this isomer than in any of the others.

The N–H and *meso*-H chemical shifts of the mixed pyrrole-substituted isomers summarized in Table II show interesting trends. The chemical shift, and hence the ring-current shielding, of the N–H protons is affected considerably by β-substitution. Except for *cis*-$E_4A_4PH_2$, electron-donating substituents appear to strengthen the shielding effect of the ring current while electron-withdrawing substituents appear to diminish its shielding effect. For the N–H signals of $OEPH_2$ and $OAPH_2$, this amounts to a difference in chemical shift of 0.36 ppm, with $OAPH_2$ having its N–H signal less highly shielded. The reciprocal ring current effect is noted in the *meso*-H signals of these two symmetrical porphyrins, although the effect on the *meso*-H chemical shift is considerably smaller (0.07 ppm). The extremely small differences in chemical shifts observed for the very dilute ~94% (16:1) sample of *cis*-$E_4A_4PH_2$, and similarly small shifts of dilute samples of other isomers indicate that aggregation does not play a significant role in the observed ring current shifts. From the data in Table II, the uniqueness of the *cis*- and *trans*-$E_4A_4PH_2$ becomes immediately apparent. The *trans* isomer appears to have a stronger ring current than any of the other porphyrins, based upon the N–H shift, while the *cis* isomer has by far the weakest, as already discussed above. The dramatic shift to lower shielding of the N–H protons of the *cis* isomer suggests a partial destruction of the ring current due to the unsymmetrical electron density

---

[37] (a) Hickman, D. L.; Goff, H. M. *J. Am. Chem. Soc.* **1984**, *106*, 5013. (b) Godziela, G. M.; Kramer, S. K.; Goff, H. M., *Inorg. Chem.* **1986**, *25*, 4286.

[38] (a) Smith, K. M.; Langry, K. C.; deRopp, J. S. *J. Chem. Soc., Chem. Commun.* **1979**, 1001. (b) Smith, K. M.; Langry, K. C. *J. Chem. Soc., Perkin Trans. 1* **1983**, 439.

[39] Balch, A. L.; Latos-Grazynski, L.; Noll, B. C.; Olmstead, M. M.; Zovinka, E. P. *Inorg. Chem.* **1992**, *31*, 2248.

Table III. ^1H NMR Isotropic Shifts,[a] δ, in ppm, of the (porphyrin)FeCl Complexes in $CDCl_3$ at 25 °C

complex	*meso*-H (width)	$-CH_2$CH$_3$	$-$CH$_2CH_3$	$-C(O)-N(CH_2$CH$_3)_2$	$-C(O)-N($CH$_2CH_3)_2$
(OEP)FeCl	−65.5 (900 Hz)	36.2, 39.9	4.9		
E_6A_2PFeCl	−66 (1000 Hz)	42.2(1), 40.2(2), 39.4(1), 38.0(1),	4.7	2.4^d	1.6, -0.1^c
	−71 (1000 Hz)	37.1(2), 36.6(2), 35.9(2), 34.9(1)^{b,c}			
(*t*- and *c*-)E_4A_4PFeCl	−70 (1600 Hz)	40.7, 39.4, 38.7, 36.3, 35.3	4.8	2.4^d	1.9, 1.7, -0.5^c
(OAP)FeCl	−71 (1800 Hz)			2.4^d	1.4, -0.2^c

[a] Isotropic shift = δ(obs) − δ(free base). Free base chemical shifts taken from Table II. [b] Isotropic shift calculated from the weighted average of free base ethyl methylene signals. [c] Relative intensity in parentheses. [d] Isotropic shift calculated from the weighted average of free base amide methylene signals. [e] Isotropic shift calculated from the average of free base amide methyl signals.

distribution within the porphyrin ring, caused by the unequal inductive effect exerted by the substituents. This appears to lead to cancellation of some of the ring current effect in the *cis* isomer, which causes the N–H protons to be less shielded and the *meso* protons less deshielded than those of the other octasubstituted porphyrins of this study.

Additional conclusions with regard to the location of the N–H protons can be drawn from inspection of their chemical shifts (Table II). There has been considerable interest in the rate and mechanism of N–H tautomerism in porphyrins.[40–52] The general conclusion reached by previous investigators is that the N–H protons prefer to be on opposite, rather than adjacent, pyrrole nitrogens. If that is the case, then the N–H chemical shifts of $E_6A_2PH_2$ and *trans*-$E_4A_4PH_2$ suggest that the equilibrium lies far in the direction of the protons binding to nitrogens in diethylpyrrole rings, because of the similarity of the N–H chemical shift to that of $OEPH_2$. However, the major tautomeric form of $E_2A_6PH_2$ probably has one proton on a nitrogen atom of a diethylpyrrole ring and the other on the opposite bis(*N*,*N*-diethylcarbamoyl)pyrrole nitrogen, since the observed N–H chemical shift is almost exactly intermediate between the N–H chemical shifts of $OEPH_3$ and $OAPH_2$. In the case of *cis*-$E_4A_4PH_2$, two N–H peaks are observed. This is presumably due to the fact that if the two N–H protons are on opposite nitrogens, one must of necessity be on a diethylpyrrole nitrogen and the other on a bis(*N*,*N*-diethylcarbamoyl)pyrrole nitrogen, even if tautomerism occurs. However, the observation of two N–H peaks (and four *meso*-H peaks) requires that tautomerism among *all four* nitrogens be slow on the NMR time scale. NMR investigations of the temperature dependence of both the N–H and the three *meso*-H signals of *cis*-$E_4A_4PH_2$ showed that no broadening or coalescence occurred at temperatures up to 100 °C in toluene-d_8. Hence, even at this temperature, N–H tautomerism is slow on the NMR time scale. A recent study by Ogoshi and co-workers[52] reports that mono-*meso*-substituted octaalkylporphyrins, where the *meso*-substituent is a naphthyl group, exhibit extremely slow N–H tautomerism. In this case, coalescence of the two N–H resonances occurs at somewhat above 100 °C at 270 MHz. An earlier 60-MHz NMR investigation of natural porphyrin derivatives reported that mesoporphyrin IX dimethyl ester has two N–H peaks of equal intensity at −4.48 and −4.62 ppm.[9] Another related system is 2,4-bis(2-carboxycyclopropyl)deuterioporphyrin IX, which also has two N–H peaks at 60 MHz.[8] Thus, it appears that for many porphyrins having adjacent pyrrole rings carrying electron-withdrawing groups or those having one unique *meso* substituent, the possibility exists that two N–H resonances will be observed, and even that the rate of N–H tautomerism may be very slow at room temperature.

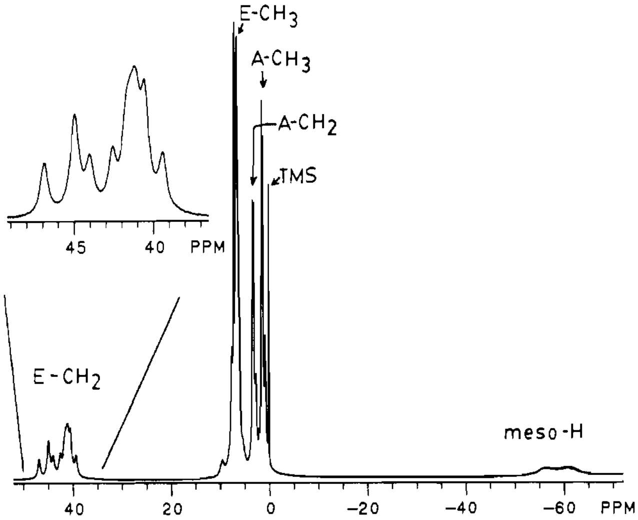

Figure 3. 300-MHz 1-D proton NMR spectrum of E_6A_2PFeCl in $CDCl_3$ at 25 °C.

High-Spin Iron(III) Porphyrin Complexes. The high-spin complexes of the type PFeCl, where P = porphyrin, are found to have large negative isotropic shifts of the *meso* protons and positive isotropic shifts of the methylene protons of the directly-bound ethyl groups (E), consistent with earlier studies of (OEP)FeCl in chlorinated hydrocarbons.[10,11,53] The excessive line widths of the *meso*-H signals precluded observation of splitting due to the lowered symmetry of the mixed-pyrrole isomers, except in the case of E_6A_2PFeCl, whose ^1H NMR spectrum is shown in Figure 3. As *N*,*N*-diethylcarbamoyl groups are substituted for ethyl, the magnitude of the isotropic shifts of the *meso* protons of the high-spin complexes increases, as summarized in Table III. This is consistent with the expectation that electron-withdrawing substituents on the periphery of the porphyrin tend to increase the degree of metal to ligand (M → L) π-back-bonding. This places larger π-spin density into the empty $4e(\pi)$ orbitals[10,11,53] and thus on the *meso* carbons.

The E–CH_2 signals of the chloroiron(III) complexes of the mixed pyrrole isomers were expected to consist of multiple peaks due to (1) diastereotopism of the methylene protons (as also observed for (OEP)FeCl[10,11,53]), since none of the chloroiron(III) porphyrins have a horizontal plane of symmetry, and (2) the likelihood of slightly different σ-delocalization to E–ethyl groups which have different nearest and next-nearest neighbors. Thus, *cis*-E_4A_4PFeCl was expected to have four E–CH_2 signals, *trans*-E_4A_4PFeCl was expected to have two, and E_6A_2PFeCl was

---

(40) Storm, C. B.; Teklu, Y. *J. Am. Chem. Soc.* **1972**, *94*, 1745.
(41) Storm, C. B.; Teklu, Y.; Sokolski, E. A. *Ann. N.Y. Acad. Sci.* **1973**, *206*, 631.
(42) Abraham, R. J.; Hawkes, G. E., Smith, K. M. *Tetrahedron Lett.* **1974**, 1483.
(43) Eaton, S. S.; Eaton, G. R. *J. Am. Chem. Soc.* **1977**, *99*, 1601.
(44) Gust, D.; Roberts, J. D. *J. Am. Chem. Soc.* **1977**, *99*, 3637.
(45) Henning, J.; Limbach, H. H. *J. Am. Chem. Soc.* **1984**, *106*, 292.
(46) Limbach, H. H.; Kendrick, R.; Yannoni, C. S. *J. Am. Chem. Soc.* **1984**, *106*, 4059.
(47) Butcher, R. J.; Jameson, G. B.; Storm, C. B. *J. Am. Chem. Soc.* **1985**, *107*, 2978.
(48) Crossley, M. J.; Harding, M. M.; Sternhell, S. *J. Am. Chem. Soc.* **1986**, *108*, 3608.
(49) Crossley, M. J.; Field, L. D.; Harding, M. M.; Sternhell, S. *J. Am. Chem. Soc.* **1987**, *109*, 2335.
(50) Frydman, L.; Olivieri, A. C.; Diaz, L. E.; Frydman, B.; Morin, F. G.; Mayne, C. L.; Grant, D. M.; Adler, A. D. *J. Am. Chem. Soc.* **1988**, *110*, 336.
(51) Butenhoff, T. J.; Moore, C. B. *J. Am. Chem. Soc.* **1988**, *110*, 8336.
(52) Asakawa, M.; Toi, H.; Aoyama, Y.; Ogoshi, H. *J. Org. Chem.* **1992**, *57*, 5796.
(53) La Mar, G. N.; Eaton, G. R.; Eaton, S. S.; Holm, R. H.; Walker, F. A. *J. Am. Chem. Soc.* **1973**, *95*, 63.

expected to have six E-CH_2 signals of equal intensity. The fact that eight signals are observed for this isomer, with relative signal intensities of 1:2:1:1:2:2:2:1 (Figure 3 insert) suggests that a third factor is also very important: The out-of-plane orientation of the amide groups (A) caused by steric crowding. If one of the diethylcarbamoyls has its alkyl groups on the same side of the porphyrin plane as the chloride and the other on the opposite side, or if both sets of diethylcarbamoyl alkyl groups are on the same side of the porphyrin plane as the chloride in half the molecules and on the opposite side in the other half, then the E–ethyl substituents adjacent to each of these diethylcarbamoyl groups will be diastereotopic due to two different effects. Thus, twelve unique environments for the E–CH_2 protons are created. Space-filling models (CPK) suggest that on the basis of steric crowding, the "up–down" diethylcarbamoyl isomer should be favored over the "two-up" or "two-down" isomers. Attempts to completely assign the E–CH_2 resonances of E_6A_2PFeCl by COSY and NOESY techniques were unsuccessful due to the short relaxation times of the E–CH_2 protons ($T_2^* < 3$ ms, $T_1 = 2$–4 ms), which may have inhibited the detection of cross peaks, and by the overlap of their signals (Figure 3 insert).

Only a small positive isotropic shift is experienced by the A–CH_2 protons, since the contact shift is rapidly attenuated as the number of σ bonds between the methylene protons and the porphyrin ring increases. (The A–CH_2 protons are one bond further removed from the porphyrin ring than are the E–CH_3 protons. Hence it is not surprising that the isotropic shifts of the A–CH_2 protons are smaller than for the E–CH_3 protons.) The breadth of the A–CH_2 signal precludes any observation of diastereotopism of these protons or differentiation of the *syn* and *anti* environments resulting from restricted rotation about the amide C(O)–N bond. In contrast, the A–CH_3 protons have extremely small isotropic shifts and the signals are sharp enough that it is possible to see the *syn* and *anti* A–CH_3 resonances resulting from restricted rotation about the amide bond, as was observed for the diamagnetic free base porphyrins, discussed above. Indeed, the isotropic shifts reported in Table III were calculated from the chemical shifts of the two peaks, ~3.1 and 0.9 ppm, assuming that the two signals have the smallest possible isotropic shifts and hence have not switched order from those of the free base precursors. However, the *absolute* assignment of the signals of the *syn* and *anti* groups has not been made for any of the compounds in this study.

Low-Spin Iron(III) Complexes: Proton NMR Spectroscopy. Upon addition of *N*-methylimidazole to the high-spin PFeCl complexes, the low-spin bis(*N*-methylimidazole) adducts are formed. The proton NMR spectra of these complexes were examined over the temperature range of the solvent in $CDCl_3$ and for $[E_6A_2PFe(N\text{-}MeIm)_2]^+$ in CD_2Cl_2. Resonance assignments of the low-symmetry complexes were based on chemical shift values of the highly-symmetrical complexes of $[(OEP)Fe(N\text{-}MeIm)_2]^+Cl^-$ and $[(OAP)Fe(N\text{-}MeIm)_2]^+Cl^-$, integration of peak areas and the temperature dependences of the isotropic shifts as compared to those of $[(OEP)Fe(ImH)_2]^+Cl^-$;[54] as well as COSY and NOESY spectra in the case of $[E_6A_2PFe(N\text{-}MeIm)_2]^+$.

Complete Assignment of the ^{1}H NMR Resonances of $[E_6A_2PFe(N\text{-}MeIm)_2]^+$: a. 1-D ^{1}H NMR Spectra. In Figure 4 is shown the complete 1-D proton NMR spectrum of $[E_6A_2PFe(N\text{-}MeIm)_2]^+$ in CD_2Cl_2 at –45 °C. It can be seen that the number of peaks present is greater than the predicted number of types of protons, based on the expectation that due to rapid ligand rotation about the Fe–N bond there should be a plane of symmetry passing through the porphyrin plane. In fact, there are 11 separate peaks of relative signal intensity 2. Three of these account for the 2-, 4-, and 5-H of *N*-methylimidazole, at –8, +12, and +8 ppm, respectively, as marked in Figure 4. The remaining eight signals integrating to two protons each are due to the six inequivalent E–CH_2 protons and the two types of *meso* protons. The reason for the nonequivalence of all E–CH_2 protons (which were also found to be nonequivalent in the ^{1}H NMR spectrum of the HS Fe(III) form of this same isomer discussed above and shown in Figure 3) is again due to the fact that the amide groups are not in the plane of the porphyrin ring of this six-coordinate porphyrin complex, thus making the E–CH_2 protons diastereotopic. Again, two possibilities exist: Either both amides on average have their alkyl groups on one side of the porphyrin plane and the carbonyl groups on the other side, or one amide has its alkyl groups above and the other below the plane of the porphyrin. In either case the E–CH_2 protons are diastereotopic.

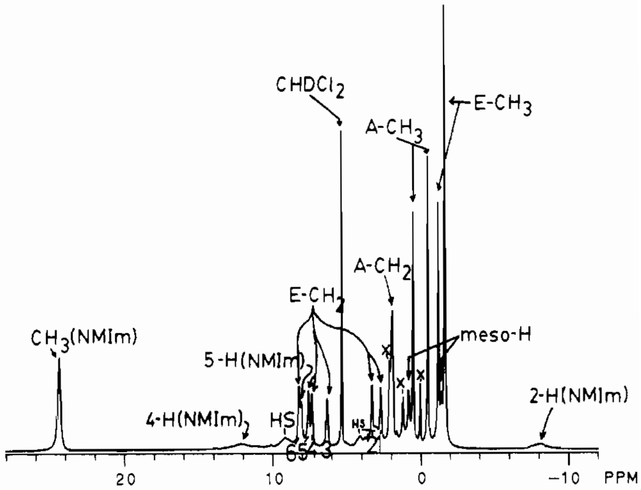

Figure 4. Complete one-dimensional ^{1}H NMR spectrum of $[E_6A_2PFe(N\text{-}MeIm)_2]^+$ in CD_2Cl_2 at –45 °C, recorded with a digital resolution of 1.5 Hz/point, showing the 11 peaks of integrated intensity 2. The broad peaks marked HS are due to the presence of a small amount of the high-spin complex, $[E_6A_2PFeCl]$, and several impurities are marked X.

Table IV. High-Temperature Region Slopes and Absolute Intercepts[a] of Paramagnetically Shifted Resonances of $[E_6A_2PFe(N\text{-}MeIm)_2]^+Cl^-$ in CD_2Cl_2 as Compared to Those of $[(OEP)Fe(ImH)_2]^+Cl^-$ in $CDCl_3$[b]

proton type (intens)	slope, ppm K	intercept, ppm	av slope, ppm K	av intercept, ppm
meso-H (2)	–3200	12.7	–3100	13.4
(2)	–3000	14.0		
OEP[b]			–3237	13.7
CH_3(Et) (18)	–1167	3.7	–1167	3.7
OEP[b]			–1382	4.7
CH_2(Et) (2) (H-5)	–2500	15.7	–1425	11.9
(2) (H-4)	–2500	15.5		
(2) (H-6)	–417	10.9		
(2) (H-3)	–650	10.4		
(2) (H-2)	–1233	9.5		
(2) (H-1)	–1250	9.2		
OEP[b]			–882	8.8
CH_3(A) (6)	–467	2.2	–434	1.9
(6)	–400	1.5		
CH_2(A) (4)	–382	3.6	–199	2.5
(2)	–84	2.5		
(2)	+53	1.9		
N-CH_3(L) (6)	6300	–3.1	6300	–3.1
2-H(L) (2)	–2233	1.8	–2233	1.8
4-H(L) (2)	3217	–2.1	3217	–2.1
5-H(L) (2)	–617	~9.9	–617	~9.9

[a] Uncorrected for diamagnetic shift. [b] Taken from ref 54.

In Figure 5 is shown the temperature dependence of the proton resonances of $[E_6A_2PFe(NMeIm)_2]^+$ in CD_2Cl_2 from +40 to –90 °C. Analysis of this modified Curie plot shows that the temperature dependences of the six diastereotopic E–CH_2 resonances behave in a pairwise fashion, with resonance pairs H-1 and H-2, H-3 and H-6, and H-4 and H-5 having very similar

---

(54) La Mar, G. N.; Walker, F. A. *J. Am. Chem. Soc.* **1973**, *95*, 1782.

Table V. Isotropic Shifts of the $[(\text{porphyrin})\text{Fe}(N\text{-MeIm})_2]^+\text{Cl}^-$ in $CDCl_3$ at –30 °C[a]

porphyrin	*meso*-H[b]	$–CH_2CH_3$[b]	$–CH_2CH_3$[b]	$–C(O)N(CH_2CH_3)_2$[b]	$–C(O)N(CH_2CH_3)_2$[b]	$N–CH_3$- (L)	2-H- (L)	4-H- (L)	5-H- (L)
OEP	–6.7 (4)	1.9 (16)	–3.02 (24)			18.7	–14.5	3.4	1.5
E_6A_2P[c]	–10.2 (2), –8.4 (2)	–1.4 (2), –1.2 (2), 1.4 (2), 3.4 (2), 4.3 (4)	–3.3 (18)	–1.7 (8)	–2.1 (6), –1.6 (6)	19.6	–16.2	3.8	0.8
t-E_4A_4P[d]	–9.9 (4)	–1.04 (4), 0.4 (4)	–3.8 (12)	–1.9 (8), –1.5 (8)	–1.4 (12), –0.8 (12)	21.0	–16.7	4.9	–0.4
c-E_4A_4P[d]	–10.6 (2), –8.5 (1), –8.2 (1)	–1.3 (4), 1.7 (4)	–3.2 (12)	1.9 (8), –1.5 (8)	–1.5 (12), –1.2 (12)	20.4	–15.0	4.9	1.1
OAP	–6.5 (4)			–1.4 (32)	–1.2 (24), –1.0 (24)	21.0 (br)			1.8 (br)

[a] Isotropic shift = δ(obs) – δ(free base). Free base chemical shifts taken from Table II. [b] In parentheses, intensity, in terms of number of protons. [c] Assignments based on temperature dependence and on COSY and NOESY spectra (see test and also Figures 5 and 6 and Table IV). [d] Assignments based on temperature dependence.

slopes. On the basis of the similar slopes of the pairs of E-CH_2 proton resonances labeled 1–6 in Figure 4, the geminal pairs were preliminarily assigned to be H-1 and H-2, H-3 and H-6, and H-4 and H-5. The average slope and intercept of the six E-CH_2 resonances are similar to those found for the α-CH_2 resonance of $[\text{OEPFe(ImH)}_2]^+\text{Cl}^-$ in $CDCl_3$,[54,55] as summarized in Table IV. The average slope and intercept of the two E–CH_3 resonances, of relative areas 6 and 12, are also similar to those of the CH_3 resonances of $[(\text{OEP})\text{Fe(ImH)}_2]^+\text{Cl}^-$,[54,55] as also summarized in Table IV. The temperature dependence of the two *meso*-H resonances at +0.7 and –1.5 ppm also depicted in Figure 4 also parallel each other, and their average temperature dependence follows closely that of $[(\text{OEP})\text{Fe(ImH)}_2]^+\text{Cl}^-$,[54,55] as summarized in Table IV. Similar assignments were made from the temperature dependence of the (similarly shifted) resonances of the same isomer in $CDCl_3$ and for the *cis* and *trans* isomers of $[E_4A_4\text{PFe}(N\text{-MeIm})_]^+\text{Cl}^-$ in both CD_2Cl_2 and $CDCl_3$. The isotropic shifts of all low-spin complexes (except that of $[E_2A_6\text{PFe(NMeIm)}_2]^+$), in $CDCl_3$ at -30 °C are listed in Table V.

Curvature in the Curie plot, such as that observed for the three pairs of E–CH_2 signals of $[E_6A_2\text{PFe}(N\text{-MeIm})_2]^+$ in CD_2Cl_2 (Figure 5), has previously been observed for the methyl resonances of $[(\text{protoporphyrin IX})\text{Fe(CN)}_2]^-$.[10] It is believed to be due to the hindered rotation of methyl, and especially longer-chain alkyl groups, around the porphyrin–alkyl bond as the temperature is lowered. From Figure 5 it can be seen that H-4 and H-5 are most affected by this hindrance in rotation. It will be shown below that these are the *a*-E–CH_2 protons, which are adjacent to the bulky diethylcarbamoyl substituents. Other resonances also show curvature in the modified Curie plot of Figure 5, most notably the N–CH_3 resonance of the coordinated ligands, which is also likely due to hindered rotation of the axial ligand, as observed previously for other tetraphenylporphyrin complexes.[29,56] This hindrance in rotation is consistent with the observation of NOE cross-peaks between the N–CH_3 and *a*-E–CH_3 and A–CH_3 resonances discussed below and shown in Figure S-3 (supplementary material). Assuming that all the ethyl groups and the axial ligands are freely rotating at the highest temperatures investigated, the temperature dependences of the resonances of Figure 5 were extrapolated to infinite temperature ($1/T = 0$). The slopes of these lines, also called the "high-temperature slopes", and their intercepts, are included in Table IV, together with those of $[\text{OEPFe(ImH)}_2]^+\text{Cl}^-$ in $CDCl_3$.[54] The significance of these "high-temperature slopes" and intercepts will be discussed further after presentation of the complete assignment of the resonances by COSY and NOESY techniques.

b. 2-D ^{1}H NMR Spectra. In order to unambiguously assign all E–CH_2, E–CH_3, and *meso*-H resonances of $[E_6A_2\text{PFe}(N\text{-MeIm})_2]^+$ an extensive investigation of the COSY and NOESY spectra at various temperatures was undertaken. Due to dipolar relaxation between the electron spin of the single unpaired electron of low-spin Fe(III) and the protons of interest, the spin-lattice and spin-spin relaxation times, T_1 and T_2^*, respectively, of the protons are very short[57] (although not as short as those of derivatives of $[(\text{TPP})\text{Fe}(N\text{-MeIm})_2]^+$, where the β-pyrrole substituents are protons that are directly attached to the π system into which spin density is delocalized[27]). In addition, both T_1 and T_2^* values become shorter as the temperature is lowered. As a consequence of the short relaxation times the spectral parameters for both the COSY and NOESY experiments need to be optimized, carefully adjusted and fine-tuned to the particular

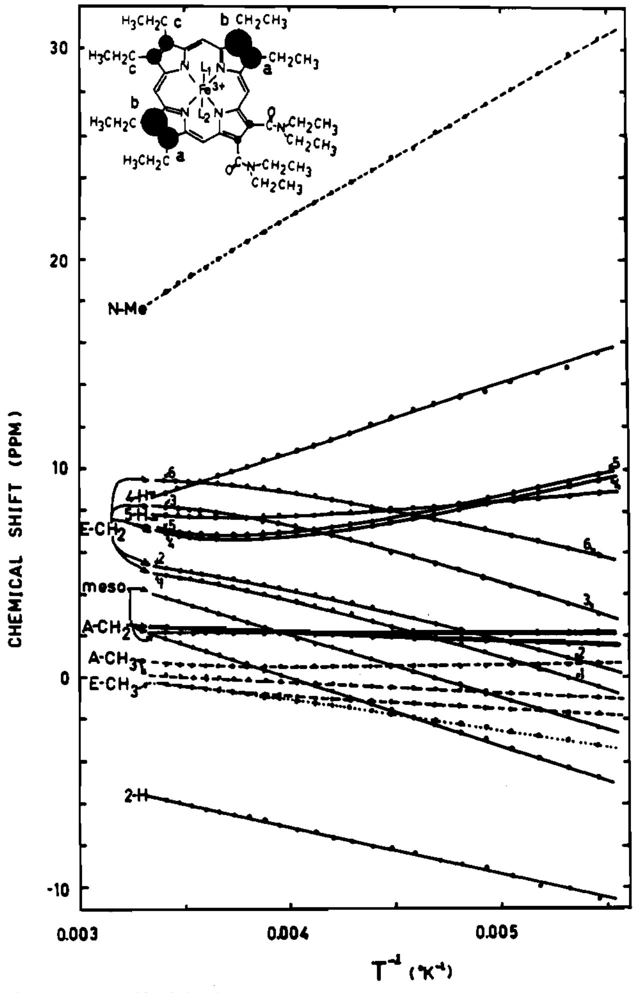

Figure 5. Modified Curie plot (not corrected for the diamagnetic shifts) for the protons of $[E_6A_2\text{PFe}(N\text{-MeIm})_2]^+\text{Cl}^-$ in CD_2Cl_2. Inset: Structure of the complex and superimposed schematic diagram (modified from that of Longuet-Higgins et al.[3] by the expected electron-donating effect of the E groups and electron-withdrawing effect of the A groups) of the electron density distribution in the orbital into which the unpaired electron is delocalized by P→Fe π-back-bonding.

---

(55) It has been shown previously for a series of unsymmetrically substituted $[(\text{TPP})\text{Fe}(N\text{-MeIm})_2]^+\text{Cl}^-$ complexes,[26] that despite the range of individual pyrrole-H resonances, the average slope and intercept obtained from the Curie plot vary only slightly for a wide range of unsymmetrically substituted porphyrins. Apparently this is also true of α-CH_2 and *meso*-H resonances of β-pyrrole-substituted porphyrin complexes.

(56) Walker, F. A.; Simonis, U. *J. Am. Chem. Soc.* **1991**, *113*, 8652.

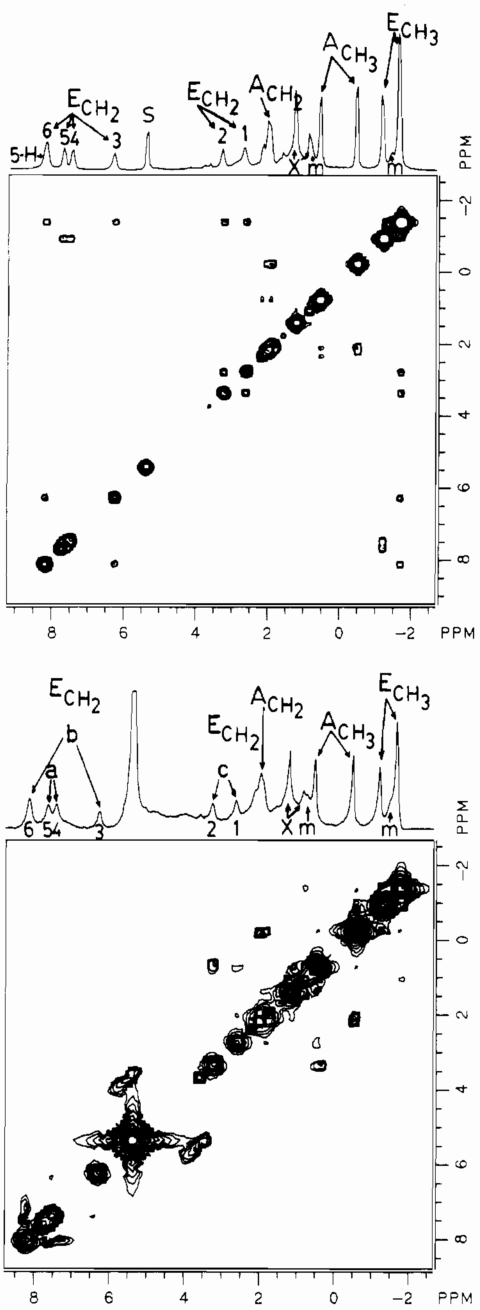

Figure 6. Top: (a) COSY spectrum of $[E_6A_2PFe(N\text{-MeIm})_2]^+Cl^-$ in CD_2Cl_2 at −45 °C. Bottom: (b) NOESY spectrum of $[E_6A_2PFe(N\text{-MeIm})_2]^+Cl^-$ at −45 °C, obtained using an optimized mixing time of 21 ms. Impurities are marked X.

T_1 and T_2^* values of the protons of interest, as we[11,27,56] and others[58,59] have discussed recently. With respect to the COSY experiments reported herein, the acquisition time in t_2 was chosen to be of the order of $1.5T_2^*$ (longest T_2^* = 13 ms) and was set to 19.7 ms to give a final digitization of 50 Hz/point. The COSY map obtained under these conditions at −45 °C is shown in Figure 6a. This temperature was chosen to enhance signal dispersion and minimize resonance overlap, as is evident both from the 1-D spectrum of Figure 4 and the Curie plot of Figure 5 at $1/T = 4.34 \times 10^{-3}$ K^{-1}.

It can be seen in the COSY spectrum (Figure 6a) that the E–CH$_2$ peaks of relative signal intensity 2 at 7.69 and 6.27 ppm (labeled 5 and 4) are coupled to each other and to the E–CH$_3$ peak of area 6 at −1.23 ppm. The E–CH$_2$ resonances of intensity 2 at 8.15 and 6.27 ppm (labeled 6 and 3) and those at 3.25 and 2.62 ppm (labeled 2 and 1) are all coupled to the E–CH$_3$ resonance of intensity 12 at −1.70 ppm. The broad A–CH$_2$ resonance (line width 0.4 ppm) is seen from the COSY spectrum to be composed of two closely-spaced, overlapping pairs of resonances, one of which is coupled to the A–CH$_3$ peak at −0.51 ppm and the other to that at 0.50 ppm. Thus, the COSY spectrum provides unambiguous assignment of all diastereotopic methylene proton pairs and their respective methyl resonances. However, from the COSY spectrum alone it is not possible to determine which of the E–CH$_2$ groups is adjacent (*a*), next-adjacent (*b*), or farthest (*c*) away from the amide substituents.

In order to determine the spatial relationship of the three types of E substituents, NOESY spectra were also acquired at −45 (Figure 6b) and −60 °C (supplementary Figure S-2). These temperatures were chosen in order to suppress axial ligand exchange, which often yields spurious chemical exchange cross peaks in the NOESY spectra of paramagnetic model hemes,[60,61] as well as to minimize overlap between resonances of interest. Mixing times were varied in order to optimize the intensities of cross peaks. It was found that the optimal mixing times were generally those approximately equal to the shortest T_1 of the protons which exhibit cross correlations. The NOESY spectrum at −45 °C, acquired with a mixing time of 21 ms (Figure 6b), exhibits strong NOE cross-peaks between E–CH$_2$ resonances labeled 5 and 6, suggesting that H-5 is close to H-6. Weaker sets of cross-peaks between H-6 and H-4 and yet weaker sets between H-4 and H-3 again indicate the close proximity of these protons. These cross-correlations most likely arise from E–CH$_2$ resonances of ethyl groups that are within the same pyrrole ring, some of which may be sampling several up–down conformations on the NMR time scale.

At the low-frequency end of the NOESY spectrum of Figure 6b, the E–CH$_3$ resonance of relative intensity 6 at −1.23 ppm and the A–CH$_3$ resonance at −0.51 ppm show strong cross-correlations. The A–CH$_3$ resonance at −0.51 ppm has slightly weaker cross-peaks to the E–CH$_3$ peak of relative intensity 12 at −1.70 ppm. These latter cross-peaks suggest that this amide group is also in close proximity to another E–CH$_3$ group, as will be discussed below. In addition to these cross-peaks, the full NOESY spectrum of $[E_6A_2PFe(NMeIm)_2]^+Cl^-$, from which Figure 6b is the expansion, shows cross-peaks between the methyl resonance of the coordinated *N*-methylimidazole ligands and both the E–CH$_3$ peak of intensity 6 and the same A–CH$_3$ resonances (Figure S-3, supplementary material). These cross-peaks suggest that the *N*–CH$_3$ group is in close proximity to these two different methyl groups. That the E–CH$_3$ resonance of intensity 6 at −1.23 ppm is due to the E–CH$_3$ nearest the amide substituents is consistent with the fact that this group is in a unique magnetic environment, due to its spatial proximity to the amide substituents. Since H-4 and H-5 are *J*-coupled to this E-CH$_3$ peak of area 6 (Figure 6a), these two E-CH$_2$ resonances must represent the *a* environment, shown in the inset of Figure 5. This assignment is also consistent with the large curvature in the temperature dependence of these resonances, discussed above and shown in Figure 5. Since H-4 and H-5 have NOESY cross-correlations to H-6, it may also be concluded that H-3 and H-6 represent the *b* environment. Consistent with this, H-1 shows weak NOE cross-peaks to the *meso*-H resonance at +0.7 ppm; H-2 shows cross-peaks either to

---

(57) T_1 and T_2, respectively, of H's of $[E_6A_2PFe(NMeIm)_2]^+$ at −45 °C (chemical shift in parentheses): E–CH$_3$ (−1.70 ppm) 33, ~8 ms; *meso*-H (−1.5 ppm) 10, ~3 ms; E–CH$_3$ (−1.33 ppm) 29, ~8 ms; A–CH$_3$ (−0.51 ppm) 72, ~6 ms; A–CH$_3$ (+0.50 ppm) 29, ~11 ms; *meso*-H (+0.7 ppm) 12, ~3 ms; A–CH$_2$ (2.05 ppm) 36, ~5 ms; A–CH$_2$ (2.13 ppm) 14, ~5 ms; E–CH$_2$: H-1 (2.62 ppm) 25, ~13 ms; H-2 (3.25 ppm) 25, ~4 ms; H-3 (6.27 ppm) 29, ~8 ms; H-4 (7.44 ppm) 29, ~4 ms; H-5 (7.89 ppm) 25, ~4 ms; H-6 (8.15 ppm) 26, ~6 ms.

(58) Emerson, S. D.; La Mar, G. N. *Biochemistry* **1990**, *29*, 1545.

(59) La Mar, G. N.; de Ropp, J. S. NMR Methodology for Paramagnetic Proteins. In *NMR of Paramagnetic Molecules*; Berliner, L. J., Reuben, J., Eds.; Plenum: New York, 1993; Vol. 12, in press.

(60) Simonis, U.; Lin, Q.; Walker, F. A. Unpublished work.

(61) Lin, Q. M.S. Thesis, San Francisco State University, 1992.

this *meso*-H or to the A–CH_3 resonance with which it overlaps. (Cross-peaks between H-2 and an A-CH_3 resonance would be inconsistent with H-1 and H-2 being farthest from the amide groups. NOESY spectra recorded at –60 °C, where the *meso*-H and A–CH_3 signals do not overlap, do not show cross-peaks between H-2 and A–CH_3, as shown in Figure S-2 of the supplementary material. Unfortunately, at this temperature the T_1 of the *meso*-H is very short, and it was not possible to observe any *meso*-H cross peaks with other resonances at –60 °C.) Additional cross-peaks are observed between the A–CH_2 resonances and the A–CH_3 resonance at –0.51 ppm, but no NOE cross-peaks are observed between the A–CH_2 resonances and the A–CH_3 resonance at +0.50 ppm.

From a combination of COSY and NOESY spectra (Figures 6a,b and S-2), as discussed above, the E–methylene signals H-4 and H-5 are assigned to ethyl *a*, H-3 and H-6 to *b*, and H-1 and H-2 to *c*, as marked in the inset of Figure 5. On the basis of space-filling molecular models (CPK), one A–CH_3 group can be close enough to touch the *a*-E–CH_3 groups of the closest diethylcarbamoyl in some conformations (if they are located on the same side of the porphyrin plane) or come within 2 Å of the more distant diethylcarbamoyl on the same side of the plane, and they can approach to within 2 Å of the *b*-E–CH_3 groups if both the A- and *b*-E–ethyls are on the same side of the porphyrin plane. This close approach can account for the observed cross-peaks between the A–CH_3 resonance at –0.51 ppm and the E–CH_3 peak of area 12 at –1.70 ppm. This suggests an up, down, up relationship of the A–ethyl, *a*-E–ethyl and *b*-E–ethyl substituents, and an up, down relationship of the two *N,N*-diethylcarbamoyl groups to each other. This leads to the overall C_2 symmetry of the molecule displayed by the ^{1}H NMR spectra of Figures 4 and 6.

c. The Pattern of Spin Delocalization. The assignment of *a*-, *b*- and *c*-E–CH_2 resonances is consistent with the expected electron density distribution in the $3e(\pi)$ orbital[3] that contains the unpaired electron, shown schematically in the insert of Figure 5. This orbital is derived from the one (of the two degenerate orbitals[3]) that places small electron density at the pyrrole positions to which the electron-withdrawing amide substituents and the *c*-ethyl groups are attached. The amount of electron density at the pyrrole positions to which the *b*- and *c*-ethyl groups are attached have been empirically increased at the expense of the electron density at the pyrrole positions to which the amides are attached. The orbital model is only schematic, since it is difficult to quantify the spin density distribution based upon the E–CH_2 shifts. At the temperatures at which COSY and NOESY maps were acquired, at least some of the E–CH_2 groups are undoubtedly quite hindered in rotation. Their preferred orientation at these low temperatures is expected to lead to hyperfine shifts that are based both on the angle θ between the p_z orbital containing spin density and the dihedral angle of the methylene proton[62] and on the amount of spin density in that p_z orbital. It is not possible to separate these two contributions, due to the curvature of the Curie plots of the E–CH_2 protons, Figure 5. Analysis of the intercepts obtained by linearly extrapolating the high temperature shifts to $1/T = 0$, assuming that in the temperature range of 30–40 °C the ethyl groups and axial ligands are freely rotating, shows that while the intercepts of the E- and A–CH_3 resonances are near their diamagnetic positions, those of the E–CH_2 and the N–CH_3 of the coordinated ligands deviate by up to 11 ppm from those of their diamagnetic positions. This suggests either (1) that the E–ethyl groups and axial ligands are not freely rotating at 30–40 °C, and/or (2) that the percent spin density population of the two $3e(\pi)$ orbitals is still changing at the highest temperatures investigated.[11] However, we can say qualitatively that the similarity in the average slopes and intercepts of the resonances of $[E_6A_2PFe(N\text{-MeIm})_2]^+$ in CD_2Cl_2 to those of $[(OEP)Fe(ImH)_2]^+$ in $CDCl_3$[54] indicates that there is an approximately constant amount of spin density delocalized from the paramagnetic metal to the porphyrin ring but that in the unsymmetrical porphyrin it is unequally distributed to individual positions around the ring. A similar observation has been made concerning the pattern of spin delocalization in the dicyano complexes of a series of 2,4-disubstituted deuterohemins.[63]

The *meso*-H peak(s) of the low-spin $[PFe(N\text{-MeIm})_2]^+$ complexes display the degree of multiplicity expected based on their gross molecular symmetry: two peaks for the complex of E_6A_2P, one peak for *trans*-E_4A_4P, and three peaks (1:2:1) for its *cis* isomer, as summarized in Table V. For the symmetrically octasubstituted isomers there is a slight decrease in the isotropic shift on going from OEP to OAP, but for the unsymmetrical isomers, the *meso*-H signals are shifted significantly (by several ppm) outside this narrow range. The isotropic shift of the *meso*-H of low-spin Fe(III) complexes of OEP has previously been shown to be largely dipolar in nature (estimated to be –9.3 ppm at 29 °C in $CDCl_3$),[54] which in the case of the unsymmetrical porphyrins of this study includes not only the axial $(3\cos^2\theta - 1)r^{-3}$ term, but also the rhombic $(\sin^2\theta)(\cos 2\Omega)r^{-3}$ term.[11,26,64] The axial term should be identical for *all meso*-H of a given complex, and the rhombic term is identically zero for all *meso*-H or $[E_6A_2PFe(N\text{-MeIm})_2]^+$ and $[trans\text{-}E_4A_4PFe(N\text{-MeIm})_2]^+$ (it is of opposite sign for the *meso*-H resonances of intensity 1 and that of intensity 2 for $[cis\text{-}E_4A_4PFe(N\text{-MeIm})_2]^+$). The fact that $[E_6A_2PFe(N\text{-MeIm})_2]^+$ shows large separation (~2 ppm) of the two *meso*-H peaks thus argues for the small contact term (estimated to be *+2.3 ppm* at 29 °C for $[OEPFe(ImH)_2]^+$ in $CDCl_3$[54]) being the one which causes the separation. The $3e(\pi)$ orbitals have nodal planes at the *meso* positions, and the observed contact contribution is positive, suggesting that this small contact term is σ in nature. This would suggest that the assignment of the *meso*-H resonance of the $[E_6A_2PFe(N\text{-MeIm})_2]^+$ complex at +0.7 ppm (Figure 5) as being that due to *meso*-H which have only diethylpyrrole neighbors is consistent with the expected general increase in electron density (and thus also spin density) in the regions of the porphyrin ring where electron-donating substituents are present. It is also consistent with the cross peaks observed between it and the *c*-E–CH_2, resonance H-2 (*vide supra*).

The axial ligand resonances of the $[PFe(N\text{-MeIm})_2]^+$ isomers also show interesting trends. In particular, for this discussion we will focus on the *N*-methyl signal, which has the largest isotropic shift of any proton in the low-spin Fe(III) complexes of the β-substituted porphyrins. It has previously been shown that the N–CH_3 isotropic shift is due to 60% contact and 40% dipolar contribution.[65] The *N*-methyl isotropic shift increases significantly as *N,N*-diethylcarbamoyls are substituted for ethyl groups on the periphery of the molecule (Table V), suggesting that greater spin delocalization occurs to the axial ligands as more electron-withdrawing substituents are present on the porphyrin ring. The shift is about 0.9 ppm in going from OEP to E_6A_2P and again to *cis*-E_4A_4P, but only an additional 0.6 ppm on going all the way to OAP.

It is also striking that the N-CH_3 resonance of $[OAPFe(N\text{-MeIm})_2]^+$ becomes much broader at lower temperatures than that of any of the other isomers as shown in supplementary Figure S-4. The temperature dependences of the N–CH_3 resonances of all isomers investigated show curvature with $1/T$, as shown in Figure 5 for $[E_6A_2PFe(N\text{-MeIm})_2]^+$, suggesting that rotation of the axial ligands is hindered at low temperatures. The N–CH_3

---

[62] La Mar, G. N. In *NMR of Paramagnetic Molecules*; La Mar, G. N., Horrocks, W. D., Holm, R. H., Eds.; Academic Press: New York, 1973; pp 98–100.

[63] La Mar, G. N.; Viscio, D. B.; Smith, K. M.; Caughey, W. S.; Smith, M. L. *J. Am. Chem. Soc.* **1978**, *100*, 8085.

[64] (a) Horrocks, W. D.; Greenberg, E. S. *Biochim. Biophys. Acta* **1973**, *322*, 38. (b) Horrocks, W. D.; Greenberg, E. S. *Mol. Phys.* **1974**, *27*, 993.

[65] Satterlee, J. D.; LaMar, G. N. *J. Am. Chem. Soc.* **1976**, *98*, 2804.

Table VI. EPR Data for the $[(\text{porphyrin})\text{Fe}(N\text{-MeIm})_2]^+$ Complexes in $CDCl_3$ at 8 K

porphyrin	g_1	g_2	g_3	Σg^2	V/λ^a	Δ/λ^b	V/Δ^c	$[a^2 + b^2 + c^2]^d$
OEP	2.865	2.272	1.543	15.87	2.02	3.22	0.63	0.997
E_6A_2P	2.881	2.268	1.540	15.82	1.99	3.26	0.61	0.998
t-E_4A_4P	3.001	2.227	1.505	16.23	1.78	3.55	0.50	1.010
c-E_4A_4P	2.742	2.312	1.700	15.75	2.56	3.54	0.72	1.007
OAP	2.841	2.295	1.637	15.87	2.23	3.52	0.63	1.010

[a] $V/\lambda = g_{xx}/(g_{zz} + g_{yy}) + g_{yy}/(g_{zz} - g_{xx})$.[68] The proper axis system for B-hemichromes has $g_{zz} = g_1$, $g_{yy} = g_2$, $g_{xx} = g_e$, with all values positive.[68] [b] $\Delta/\lambda = g_{xx}/(g_{zz} + g_{yy}) + g_{zz}/(g_{yy} - g_{xx}) - (1/2)V/\lambda$.[68] This parameter has been called the "tetragonality" by Blumberg and Peisach.[66] [c] V/Δ has been called the "rhombicity" by Blumberg and Peisach.[66] [d] $a = (g_{zz} + g_{yy})/4$ K; $b = (g_{zz} - g_{xx})/4$K; $c = (g_{yy} - g_{xx})/4$ K; $4\text{ K} = [8(g_{zz} + g_{yy} - g_{xx})]^{1/2}$.[68]

resonances of all but the OAP isomer broaden only very slowly below 0 °C, indicating that chemical exchange of *N*-MeIm ligands is not the cause of the extreme breadth of the N–CH_3 signal of $[\text{OAPFe(NMeIm)}_2]^+$. Both the small incremental shift of the N–CH_3 resonance on going from *cis*-E_4A_4P to OAP and the breadth of the N–CH_3 signal for the latter compound (Figure S-4) suggest that at low temperatures, and even to some extent at room temperature, $[\text{OAPFe}(N\text{-MeIm})_2]^+$ contains multiple isomeric species, probably due to differing out-of-plane orientations of the carbonyl and diethylamide parts of the substituent on adjacent pyrrole rings (four up–down; three up–down, 1 down–up; etc), which cannot interconvert rapidly on the NMR time scale, due to steric interference between the amide groups. If all four up–down rotational isomers were present in their statistically expected ratios, five N–CH_3 resonances, of relative intensities 1:2:2:2:1 could be observed. The chemical shifts of these resonances should not differ greatly and their widths could well be greater than the chemical shift differences, thus leading to the observed broad resonance envelope. It is expected that this steric crowding will be more significant in the 6-coordinate complexes than in the free base or 5-coordinate high-spin chloroiron(III) forms, since 6-coordination imposes more requirement that the porphyrin ring itself be planar. Additionally, it is also possible that, as the temperature is lowered, rotation of the axial ligands is hindered by the amide groups, producing a range of different relative orientations of the two planar axial ligands, thus changing their contact shifts slightly.

EPR Spectroscopy. The EPR spectra of the low-spin iron(III) bis(*N*-methylimidazole) porphyrin complexes of the series of pyrrole-substituted porphyrins were measured in $CDCl_3$ at 8 K. The *g* values are listed in Table VI. The parameters are typical for normal "B-hemichrome" species[66] and are quite similar among the complexes studied. The greatest differences in *g* values are between the *cis* and *trans* isomers of $[E_4A_4PFe(N\text{-MeIm})_2]^+$, shown in Figure 7, where the *trans* isomer (on the basis of signal intensity, 70%:30%) has the largest value of g_1 and the smallest value of g_3. The crystal field parameters V/Δ and Δ/λ have been calculated from the equations of Griffith,[67] as modified by Taylor[68] and are also included in Table VI. Since, at the temperature of the EPR measurements (8 K), we expect all complexes to have their most stable structures, i.e., with axial ligands in mutually parallel planes,[18,69] differences in crystal field parameters must be due to differences in substitution and symmetry in the porphyrin plane. The results are at first glance counter-intuitive: Δ/λ, the so-called tetragonality parameter of Blumberg and Peisach,[65] which has been said to be a measure of ligand basicity,[65] increases as the number of amide substituents increases, and V/Δ, the so-called rhombicity parameter is much smaller for the *trans* isomer of $[E_4A_4PFe(N\text{-MeIm})_2]^+$ than for the *cis*. The increase in the tetragonality as the number of amide groups increases is consistent with the fact that as the *porphyrin* substituents become more electron-withdrawing, the axial ligands can become stronger donors. The decrease in rhombicity is striking, in that the value of V/Δ calculated for the *cis* isomer is slightly greater than the theoretical value of $^2/_3$ required for a "proper axis system", as discussed by Taylor.[68] This suggests the possibility that, at least at the temperature of the EPR measurements (8 K), the principal magnetic axis of the *cis* isomer may be in the plane of the porphyrin rather than along the *N*-methylimidazole binding axis, as assumed for other B-type hemins,[65,68] and thus the orbital of the unpaired electron may be predominantly d_{xy} in nature. Bis(imidazole) complexes of ferric chlorins may also have such an axis system,[68,70–72] based upon their large values of V/Δ when calculated according to the traditional definition that $g_1 = g_{zz}$, $g_2 = g_{yy}$, and $g_3 = g_{xx}$.[73] However, in the absence of single-crystal EPR measurements, the direction of the principal magnetic axis cannot be assigned unambiguously. In any case, it should be noted that in previous studies of unsymmetrically *meso*-substituted tetraphenylporphyrin complexes of Fe(III)[18] no difference in the EPR spectra of *cis* and *trans* isomers of $[(p\text{-Cl})_2(p\text{-NEt}_2)_2(\text{TPP})\text{Fe}(N\text{-MeIm})_2]^+$ was observed. The fact that the pyrrole-substituted *cis* and *trans* isomers do have different EPR parameters demonstrates the much greater effect that the pattern of pyrrole substitution has upon the d-orbital energies, as reflected in the observed *g* values of low-spin Fe(III).

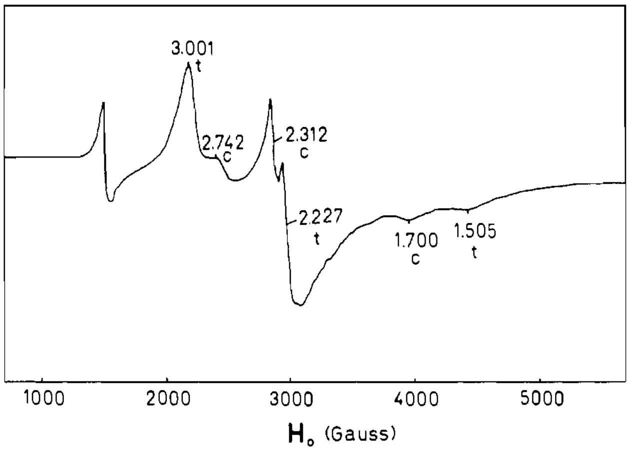

Figure 7. X-Band EPR spectrum of a 30:70 mixture of *cis* and *trans* $[E_4A_4PFe(N\text{-MeIm})_2]^+Cl^-$ in $CHCl_3$, recorded at 8 K. In addition to the two rhombic signals from low-spin Fe(III), a $g = 6$ high-spin Fe(III) signal is also observed. Although the derivative signal from this high-spin Fe(III) impurity is large in amplitude, owing to very favorable relaxation properties, its concentration is very small compared to those of the two low-spin Fe(III) species, labeled *c* (cis) and *t* (trans).

Summary. In order to vary the electron-donating and -withdrawing character of substituents on the β-pyrrole positions, six octasubstituted porphyrin isomers with either diethyl or bis(*N,N*-diethylcarbamoyl) substituents on the β positions have been synthesized and investigated by UV–visible and ^1H NMR spectroscopy. The results show that the electronic spectra of the free base porphyrins are as predicted by Falk,[1] with *cis*-E_4A_4-

---

(66) Blumberg, W. E.; Peisach, J. *Adv. Chem. Ser. A* **1971**, *100*, 271.

(67) Griffith, J. S. *Proc. R. Soc. London, Ser. A* **1956**, *235A*, 23.

(68) Taylor, C. P. S. *Biochim. Biophys. Acta* **1977**, *491*, 137.

(69) Walker, F. A.; Huynh, B. H.; Scheidt, W. R.; Osvath, S. R. *J. Am. Chem. Soc.* **1986**, *108*, 5288.

(70) Stolzenberg, A. M.; Strauss, S. H.; Holm, R. H. *J. Am. Chem. Soc.* **1981**, *103*, 4763.

(71) Safo, M. K.; Gupta, G. P.; Watson, C. T.; Simonis, U.; Walker, F. A.; Scheidt, W. R. *J. Am. Chem. Soc.* **1992**, *114*, 7066.

(72) Using a "proper" axis system, which requires the definitions $g_z = -1.700$, $g_y = 2.742$, $g_x = -2.312$,[68] yields the values $V/\lambda = 2.24$, $\Delta/\lambda = -3.68$, and $V/\Delta = -0.61$, $a^2 + b^2 + c^2 = 1.006$.

(73) Although the magnetic axes of $[cis\text{-}E_4A_4PFe(NMeIm)_2]^+$ may differ at the low temperature of the EPR spectral measurement, it is likely that the magnetic anisotropy changes with temperature in such a way as to cause NMR dipolar shifts to have the same (negative) sign, and possibly also similar magnitude, as is usually observed for low-spin Fe(III) complexes of porphyrins and chlorins.[11]

PH_2, $E_6A_2PH_2$, and $E_2A_6PH_2$ having rhodo- or nearly rhodo-type spectra, the *trans*-$E_4A_4PH_2$ isomer having an oxorhodo-type spectrum, and $OEPH_2$ and $OAPH_2$ having etio-type spectra. ^1H NMR investigations of the free base porphyrins revealed that *cis*-$E_4A_4PH_2$ has a much weaker ring current than *trans*-$E_4A_4PH_2$, based on both N–H and *meso*-H chemical shifts. In addition, one of the four *meso* protons of *cis*-$E_4A_4PH_2$, probably that located between the two diethylpyrrole groups, exchanges very rapidly with deuterium in the presence of traces of acid.

The Fe(III) complexes of the six porphyrin isomers have also been prepared and investigated in both the 5-coordinate chloroiron(III) high-spin and 6-coordinate bis(*N*-methylimidazole)-iron(III) low-spin states. In both states, ^1H NMR spectra show clearly that the bulky diethylcarbamoyl groups are not in the plane of the porphyrin ring. Complete interpretation of the spectra of the high-spin complexes are most consistent with one diethylcarbamoyl group in a given pyrrole ring having its ethyl groups above and the other below the plane of the porphyrin, thus removing the plane of symmetry expected in the 6-coordinate low-spin complexes and doubling the number of unique methylene proton environments expected for diethylpyrrole groups in the 5-coordinate high-spin complexes. The octacarbamoyl complex, $[(OAP)Fe(N\text{-}MeIm)_2]^+$, exhibits line broadening of the $N\text{–}CH_3$ resonance of the coordinated ligands at lower temperatures, perhaps due to multiple rotational isomers resulting from amide groups on adjacent pyrrole rings being on the same side or on opposite sides of the porphyrin plane, or hindered rotation of the *N*-methylimidazole ligands, or both. The $[E_6A_2PFe(N\text{-}MeIm)_2]^+$ complex has been investigated in detail over the temperature range from −90 to +40 °C by 1- and 2-D NMR techniques. As a result of these studies, a qualitative map of the spin density distribution around the porphyrin ring has been obtained. This map clearly shows that major redistribution of spin density occurs due to the presence of one pyrrole ring that has relatively electron-withdrawing substituents.

The EPR spectra of the low-spin bis(*N*-methylimidazole) complexes are all rhombic. Calculation of crystal field parameters shows that all are typical of B-hemichromes[63] except those of *cis*-$[E_4A_4PFe(N\text{-}MeIm)_2]^+$, which has a rhombicity V/Δ larger than $^2/_3$. This larger rhombicity suggests the possibility that, at least at 8 K, this complex has its principal magnetic axis in the porphyrin plane rather than along the molecular *z*-axis.

Acknowledgment. The financial support of the National Institutes of Health (Grant DK 31038) is gratefully acknowledged. The Department of Chemistry at San Francisco State University also acknowledges grants from the National Institutes of Health (RR 02684) and the National Science Foundation (DMB-8516065) for purchase of the GN-300 and QE-300 NMR spectrometers and the National Science Foundation (DMB-8507726) for purchase of the HPLC. This publication is taken in part from M.S. theses of M.F.I. (1988) and Q.L. (1992), San Francisco State University.

Supplementary Material Available: Text giving complete procedures for synthesis of the two symmetrical pyrroles, **4** and **7**, and the symmetrical porphyrins $OEPH_2$ (**8a**) and $OAPH_2$ (**8f**) and Figure S-1, ^1H NMR spectrum of a dilute sample of 16:1 $E_4A_4PH_2$, Figure S-2, one- and two-dimensional NOESY spectra of $[E_6A_2PFe(NMeIm)_2]^+$ in CD_2Cl_2 at −60 °C, Figure S-3, complete one- and two-dimensional NOESY spectra of $[E_6A_2PFe(NMeIm)_2]^+$ in CD_2Cl_2 at −45 °C (of which Figure 6b is the expansion), showing the cross-peak between the $N\text{–}CH_3$ of the coordinated ligands and the combination of the $E\text{–}CH_3$ peak of intensity 6 at −1.23 ppm and the $A\text{–}CH_3$ peak at −0.51 ppm, and Figure S-4, one-dimensional ^1H NMR spectra of $[OEPFe(NMeIm)_2]^+$ and $[OAPFe(NMeIm)_2]^+$ in $CDCl_3$ at −30 °C (8 pages). Ordering information is given on any current masthead page.